Gondwana Research 106 (2022) 281–302

Contents lists available at ScienceDirect

Gondwana Research

journal homepage: www.elsevier.com/locate/gr

Abdominal contents reveal Cretaceous crocodyliforms ate dinosaurs

Matt A. White [a,b,*], Phil R. Bell [a], Nicolás E. Campione [a], Gabriele Sansalone [a], Sienna A. Birch [a], Joseph J. Bevitt [c], Ralph E. Molnar [d], Alex G. Cook [b], Stephen Wroe [a], David A. Elliott [b]

[a] Palaeoscience Research Centre, University of New England, Armidale 2351, New South Wales, Australia
[b] Australian Age of Dinosaurs Museum of Natural History, The Jump-Up, Winton 4735, Queensland, Australia
[c] Australian Centre for Neutron Scattering, Australian Nuclear Science and Technology Organisation, Lucas Heights 2234, New South Wales, Australia
[d] University of California Museum of Paleontology, University of California, Berkeley, CA, USA

ARTICLE INFO

Article history:
Received 23 June 2021
Revised 7 January 2022
Accepted 31 January 2022
Available online 10 February 2022
Handling Editor: J.G. Meert

Keywords:
Confractosuchus sauroktonos
Crocodyliform
Crocodylians
Morphometrics
Winton Formation
Cretaceous
Ornithopod
Stomach contents

ABSTRACT

Crocodylians are among Earth's most successful hyper-carnivores, with their crocodyliform ancestors persisting since the Triassic. The diets of extinct crocodyliforms are typically inferred from distinctive bite-marks on fossil bone, which indicate that some species fed on contemporaneous dinosaurs. Nevertheless, the most direct dietary evidence (i.e. preserved gut contents) of these interactions in fossil crocodyliforms has been elusive. Here we report on a new crocodyliform, *Confractosuchus sauroktonos* gen. et sp. nov., from the Cenomanian (92.5–104 Ma) of Australia, with exceptionally preserved abdominal contents comprising parts of a juvenile ornithopod dinosaur. A phylogenetic analysis recovered *Confractosuchus* as the sister taxon to a clade comprising susisuchids and hylaeochampsids. The ornithopod remains displayed clear evidence of oral processing, carcass reduction (dismemberment) and bone fragmentation, which are diagnostic hallmarks of some modern crocodylian feeding behaviour. Nevertheless, a macro-generalist feeding strategy for *Confractosuchus* similar to extant crocodylians is supported by a morphometric analysis of the skull and reveals that dietary versatility accompanied the modular assembly of the modern crocodylian *bauplan*. Of further interest, these ornithopod bones represent the first skeletal remains of the group from the Winton Formation, previously only known from shed teeth and tracks, and may represent a novel taxon.

© 2022 The Author(s). Published by Elsevier B.V. on behalf of International Association for Gondwana Research. This is an open access article under the CC BY-NC-ND license (http://creativecommons.org/licenses/by-nc-nd/4.0/).

1. Introduction

Modern crocodiles are numerical relicts (Simpson, 1944), the surviving members of a once more speciose group. By contrast, Mesozoic crocodyliforms occupied a far greater range of feeding ecologies including dietary extremes such as herbivory and durophagy (Buckley et al., 2000; Melstrom and Irmis, 2019).

Typically, interpreting the diets of these extinct taxa relies on tooth and skull morphologies (Melstrom and Irmis, 2019; Drumheller and Wilberg, 2019) or feeding traces on food items (Noto, Main and Drumheler, 2012; Boyd, Drumheller and Gates, 2013; Njau and Blumenschine, 2006). Among carnivorous forms, such dietary inferences focus on the largest members of the clade, *Sarcosuchus* and *Deinosuchus* (Schwimmer, 2002), which, at > 11 m long, were probably capable of dispatching similar-sized dinosaurians (Sereno et al., 2001; Rivera-Sylva, Frey and Guzmán-Gutiérrez, 2009). Smaller forms, such as *Orgresuchus*, which was discovered in a dinosaur nesting area, may also have fed on dinosaurs (Sellés et al., 2020), which is corroborated by tooth marks, and in one case, an embedded crocodyliform tooth found in an ornithopod bone (Boyd, Drumheller and Gates, 2013). However undeniable evidence of predation on dinosaurs has been discovered among much smaller representatives of other clades, with abdominal remains identified within a snake (sauropod hatchlings) (Wilson et al., 2010) and a mammal (juvenile *Psittacosaurus*) (Hu et al., 2005).

Preserved crocodyliform gut contents are demonstrably rare, a fact possibly exacerbated by extremely corrosive stomach acids, which is a hallmark of living crocodylians (Grigg and Kirshner, 2015). The only record of extinct crocodyliform stomach contents are: 1) a sphagesaurid crocodylomorph found within the abdominal cavity of the baurusuchid *Aplestosuchus* from the Late Cretaceous of Brazil (Godoy et al., 2014) and 2) indeterminate carbonized remains found within the gut of a 'yearling' crocodylian from the Eocene Green River Formation (Langston and Rose, 1978). Here we report on a new crocodyliform from the mid-Cretaceous

* Corresponding author at: Palaeoscience Research Centre, University of New England, Armidale 2351, New South Wales, Australia.
E-mail address: fossilised@hotmail.com (M.A. White).

https://doi.org/10.1016/j.gr.2022.01.016
1342-937X/© 2022 The Author(s). Published by Elsevier B.V. on behalf of International Association for Gondwana Research.
This is an open access article under the CC BY-NC-ND license (http://creativecommons.org/licenses/by-nc-nd/4.0/).

Winton Formation of Australia with exceptionally preserved stomach contents identified as the partial remains of a juvenile ornithopod dinosaur. These contents are the first definitive evidence of food-web interactions and the first skeletal elements of an ornithopod reported from the Winton Formation. Geometric morphometrics (GM) has proven to be a reliable indicator of feeding behaviour in extant and extinct crocodyliform species (Erickson et al., 2012; Walmsley et al., 2013; Piras et al., 2014; Molnar et al., 2015; Drumheller and Wilberg, 2019) and for the first time the results are substantiated using actual fossilised stomach contents.

2. Methods

2.1. Scanning

Visualisation of the stomach contents and most of the postcranial elements otherwise hidden by matrix, was achieved via neutron tomography, 3D segmentation and modelling. The fragments of the concretion housing *Confractosuchus sauroktonos* were scanned at the Australian Nuclear Science and Technology Organisation (ANSTO) using Imaging and Medical beamline at 100 μm. Neutron Radiography was also used on the fragment containing the abdominal contents at a 15 μm resolution.

2.2. Neutron tomography: Experimental setup and data reconstruction

This study utilised the Dingo thermal neutron radiography/tomography/imaging station, located at the 20 MW Open-Pool Australian Lightwater (OPAL) reactor (Australian Nuclear Science and Technology Organisation (ANSTO), Lucas Heights, New South Wales, Australia) to non-invasively image this specimen. The Dingo facility utilises a quasi-parallel collimated beam of thermal neutrons. For this study, a collimation ratio (L/D) of 1000 (Garbe et al., 2015) was used to ensure highest available spatial resolution, where L is the neutron aperture-to-sample length and D is the neutron aperture diameter. The field of view was set to 80×47 mm^2 with a voxel size of $15.8 \times 15.8 \times 15.8$ μm and sample-to-detector distance of 36 mm. Neutrons were converted to photons with a 30 μm thick terbium-doped Gadox scintillator screen (Gd2O2S:Tb, RC Tritec AG); photons were then detected by an Iris 15 sCMOS camera (16-bit, 5056×2960 pixels) coupled with a Makro Planar 100 mm Carl Zeiss lens. The specimen was scanned in two vertical parts. Each scan consisted of a total of 3200 equally-spaced angle shadow-radiographs obtained every 0.1125° as the sample was rotated 360° about its vertical axis with the specimen's centre of rotation shifted to 11.4 mm from the detector edge. Both dark (closed shutter) and beam profile (open shutter) images were obtained for calibration before initiating shadow-radiograph acquisition. To reduce anomalous noise, a total of four individual radiographs with an exposure length of 16 s were acquired at each angle (Mays, Bevitt and Stilwell, 2017). Total scan time was 5 days. The individual radiographs were summed in post-acquisition processing using the Grouped ZProjector function in ImageJ v.1.51 h, normalised and stitched using IMBL Stitch on the Australian Synchrotron Computing Infrastructure and tomographic reconstruction of the 16-bit raw data performed using Octopus Reconstruction v.8.8 (Inside Matters NV), yielding virtual slices perpendicular to the rotation axis.

2.3. Digital processing

The resulting images were imported into Mimics version 20 (Materialise HQ, Leuven, Belgium) and converted into 3D surface meshes of each individual bone. These meshes were imported into Zbrush 2021.6.2 Pixologic (Pixologic Inc, California, USA), which was used to rearticulate the digital concretion fragments that also contained separate internal meshes of the bones. Bones were occasionally split between concretionary fragments, which, following realignment, could be digitally sutured back together (Fig. 1).

2.4. Phylogeny

The phylogenetic position of *Confractosuchus sauroktonos* was assessed by adding it to the phylogenetic dataset of Martin et al. (2020) which is a derivative of the Turner (2015) matrix. This matrix was selected because it has been iteratively constructed to elucidate character evolution in crocodyliforms leading up to Eusuchia (Leite and Fortier, 2018; Martin et al., 2020; Turner, 2015). The matrix was evaluated under equally weighted parsimony in TNT 1.5 (Goloboff and Catalano, 2016), using 100 replications of a driven search strategy with random and constrained sectorial searches, 100 iterations of ratcheting, 20 iterations of drifting and 5 rounds of fusing, with the analysis stopping when the same minimum length trees were found in two consecutive runs. All characters considered as ordered by Turner (2015) were treated likewise. A further round of branch swapping was performed on the set of most parsimonious trees from the driven search to ensure thorough exploration of the tree space. Bootstrap and jackknife values for each node in the strict consensus tree were calculated from 100 resampled replicates of the driven tree search strategy, with frequencies summarised using the group present/-contradicted (GC) metric in TNT. In addition, Bremer supports were calculated using the BREMER.RUN script.

2.5. Geometric morphometrics

The skull shape of *Confractosuchus* was assessed within the context of extant and extinct crocodyliforms using two previously published 2D and 3D geometric morphometric datasets (Piras et al., 2014; Drumheller and Wilberg, 2019). The 2D analysis includes a sample of 130 crocodyliform species, used to define seven ecomorphological categories across Crocodyliformes (Drumheller and Wilberg, 2019). To this dataset, we added *Confractosuchus* and *Isisfordia duncani* based on their dorsal profiles. The 3D analysis spans 26 (3 extinct) species originally used to investigate modularity and integration in the crocodylian skull (Piras et al., 2014). Only *Confractosuchus* could be incorporated into the 3D analysis.

2.5.1. GM analysis 1

Integration into the Drumheller & Wilberg (2019) dataset was done using tpsDIG2 v2.31 (Rohlf, 2018) and the R package geomorph (Adams & Collyer, 2019). The dataset includes a total of 130 taxa (26 extant) from which six landmarks and 24 sliding semi-land-marks were chosen to capture the shape of the cranium, snout, and supratemporal fossa. To this dataset, we added *Confractosuchus* and *Isisfordia*, based on their respective right sides, which were mirrored to generate fully bilaterally symmetric skulls and appended to the Drumheller & Wilberg (2019) dataset using a custom code (Appendix A).

2.5.2. GM analysis 2

Confractosuchus was also incorporated into 73 out of 90 unilateral 3D landmarks (digitized on the left side of the skull; Supplementary Data, Fig. S1) identified by Piras et al., (2014). These data were obtained from juvenile–adult specimens of 23 extant species (Alligatoridae: 157 individuals, 8 extant species; Crocodylidae: 223 individuals, 14 extant species; *Gavialis gangeticus*: 20 individuals) and 3 fossil representatives (*Voay robustus* (Brochu, 2007a), *Crocodylus ossifragus* (Dubois, 1908), and *Dollosuchoides densmorei* (Brochu, 2007b). Data from Piras et al. (2014) were

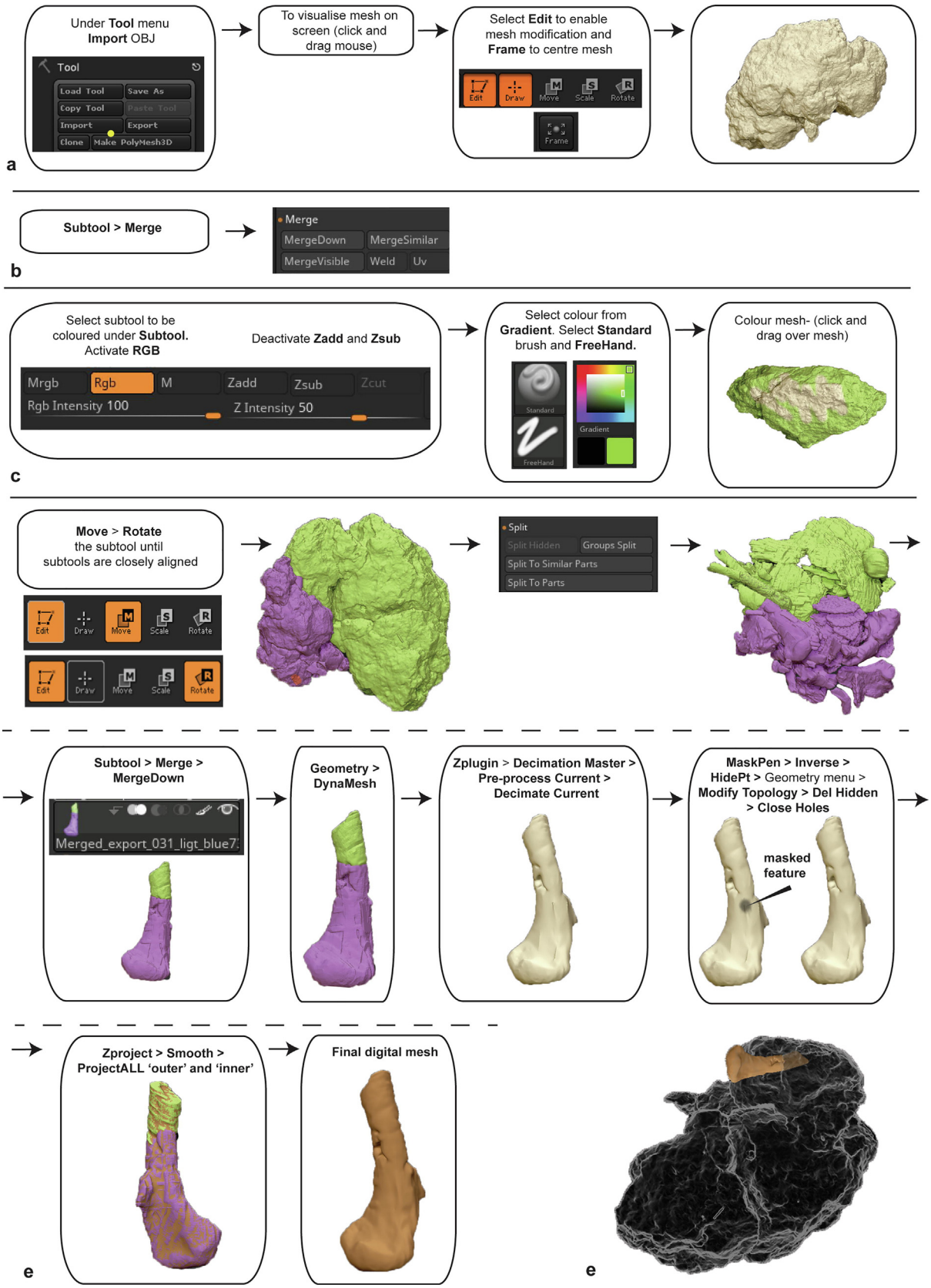

Fig. 1. Work utilizing Zbrush to digitally reconstruct and display the holotype specimen of *Confractosuchus sauroktonos* gen et sp. nov. (a) importing raw files; (b) merging subtools; (c) colouring subtools; (d) aligning concretion fragments and internal bone meshes, digitally joining bones from separate digital concretionary fragments, repairing surface artefacts of the 3D mesh files, projecting restored mesh to original raw mesh retaining original specimens' morphology; (e) digital specimen *in situ* within the digital concretionary fragment.

collected with an Immersion Microscribe G2, whereas 3D landmarks on *Confractosuchus* were digitized in the software IDAV Landmark. Successively, a generalized Procrustes analysis, has been performed in the R package "Morpho" (Schlager, 2013).

3. Descriptions and results

3.1. Systematic palaeontology

Crocodyliformes Hay 1930
Mesoeucrocodylia Whetstone & Whybrow 1983
Neosuchia Benton & Clark 1988
Eusuchia Huxley 1875
Confractosuchus gen. nov.
Type species. *Confractosuchus sauroktonos* gen. et sp. nov.
Diagnosis. As for species.

3.2. Etymology

Confractus ('broken', Latin), referring to the shattered concretion in which the holotype was preserved, and *suchus* (derived from the Greek, *Soûkhos*), referring to the Egyptian crocodile god Sobek; *sauros* ('lizard', Greek), a common word used as a suffix for dinosaur genera, and *ktonos* ('killer' Greek) referring to its abdominal contents.

3.3. Diagnosis

Neosuchian with the following autapomorphies: two pairs of longitudinal ridges on the rostrum that appear to span the prefrontal and lacrimal bones and terminate mid-rostrum; strongly regionalised vertebral assembly consisting of incipiently procoelous cervicals (c3–5), strongly procoelous thoracics (t1–2), incipiently procoelous (t3, ?t13) and amphicoelous mid-thoracic vertebrae (t4–7, ?9–12) (Fig. 2).

3.4. Holotype

AODF (Australian Age of Dinosaurs Fossil, Winton) 0890; a near-complete skull with dentition and semi-articulated postcranial skeleton missing the tail and hind limbs (Figs. 2 - 3, Supplementary Data, Fig. S2-4). It was estimated to be around 2–2.5 m in length.

3.5. Horizon and locality

Elderslie Station, Winton Shire, central-western Queensland, upper Winton Formation (Cenomanian), *ca* 93 Ma (Cook et al. 2013; Tucker et al., 2013, 2017); (AODL) Australian Age of Dinosaurs Locality 0120 (Fig. 4).

3.6. Geological and sedimentological setting.

The Winton Formation is the uppermost unit of the Eromanga Basin, part of the Great Australian Super Basin, an intracontinental sag basin, which formed during the Jurassic to Cretaceous in inland eastern Australia (Cook et al., 2013). The Winton Formation comprises labile sandstone, mudstones, claystones and minor coal all of which have been deeply weathered during the Cenozoic. The sediments originated from the Whitsundays Volcanic Province (Cook et al. 2013; Tucker et al. 2016), and were deposited in estuarine (basal), lacustrine and fluvial depositional settings. Sandstones represent high sinuosity channel and related crevasse splay deposits, whereas the mudstones and claystones represent floodplain and lacustrine deposition. Coals, silicified peat beds and richly carbonaceous shales represent peat swamp conditions in the lower part of the formation.

The holotype of *Confractosuchus sauroktonos* (AODF0890) was located *in situ* ~ 1 m below the surface during exploratory excavations of poorly-preserved sauropod remains that were found exposed on the surface within montmorillonite-rich vertisol (commonly termed black-soil), which was about 1 m thick. This layer superimposed an organic rich bluish-grey volcanogenic clay with sandstone lenses. *Confractosuchus* was located within a concretion at the transition from clay to black-soil. No additional sauropod remains were found in association with AODF0890, therefore the original relationship between the sauropod remains and those of AODF0890 are unknown; however, the sauropod remains are clearly reworked from underlying layers (Hocknull et al., 2009; White et al., 2020; Hocknull et al., 2021; Poropat et al., 2021) (Fig. 4).

3.7. Taphonomic remarks

The skeleton of *Confractosuchus* was found articulated-to-associated in life position but lacking most of the pelvic girdle, hindlimbs and the tail. The dorsal osteoderms are randomly dispersed throughout the skeleton with none *in situ*. A large cluster of osteoderms that formed the ventral shield are preserved beneath the pterygoids and cervical vertebrae and are mostly perpendicular to their life position. The skull and jaws are tightly occluding but the dentary has shifted posteriorly relative to the cranium. The pre-sacral axial skeleton is largely complete but 'segmented' into discontinuous strings of cervical and thoracic vertebrae; thoracic vertebrae 5–7 have become disarticulated and separated from their corresponding ribs, which are also scattered along with the entire gastral basket. The forelimbs are close to life position but are disarticulated; the right manus is disarticulated on the right-hand side of the rostrum whereas elements of the left manus are randomly dispersed around the left shoulder girdle (Fig. 3 and Supplementary Data, Fig. S4). There is no apparent evidence of predation/scavenging (i.e. shed teeth or tooth marks); however, this cannot be ruled out given the absence of the hind-limbs and tail, which may in itself have been the result of scavenging.

The pattern of preservation of AODF0890 is consistent with other articulated-to-associated crocodylomorph fossils in the Winton Formation (Syme and Salisbury, 2014) that were hypothesised to have been interred after a relatively brief period of subaquaeous decay in a low-energy environment (Syme and Salisbury, 2014, 2018).

Neutron tomography permitted visualisation of the abdominal cavity, revealing a remarkable insight into the diet of *Confractosuchus.* The partially-digested remains of a juvenile ornithopod dinosaur were found concentrated in the anterior part of the abdominal cavity in the vicinity of the pectoral girdle and bound unambiguously between the axial skeleton and osteoderms of the presumed gastral shield (Fig. 3; Supplementary Data, Fig. S4).

The partially-digested remains were identified as ornithopod as the femur possesses the characteristic pendant fourth trochanter, a synapomorphy of non-iguanodontian ornithopods (Norman et al., 2004). The fourth trochanter is elongate compared to other taxa, including other Australian forms (Molnar and Galton, 1986; Rich and Vickers-Rich, 1989, 1999) but is similar in extent to *Orycto-dromeus* (Brown et al., 2013).

3.8. Description of Confractosuchus sauroktonos

3.8.1. Skull

The skull (28.5 cm long, 19 cm wide) is triangular in dorsal aspect and brevirostrine (Erickson et al. 2012, see fig. 3.19 in Grigg and Kirshner, 2015), similar *Bernissartia fagesii* (see Fig. 1 in

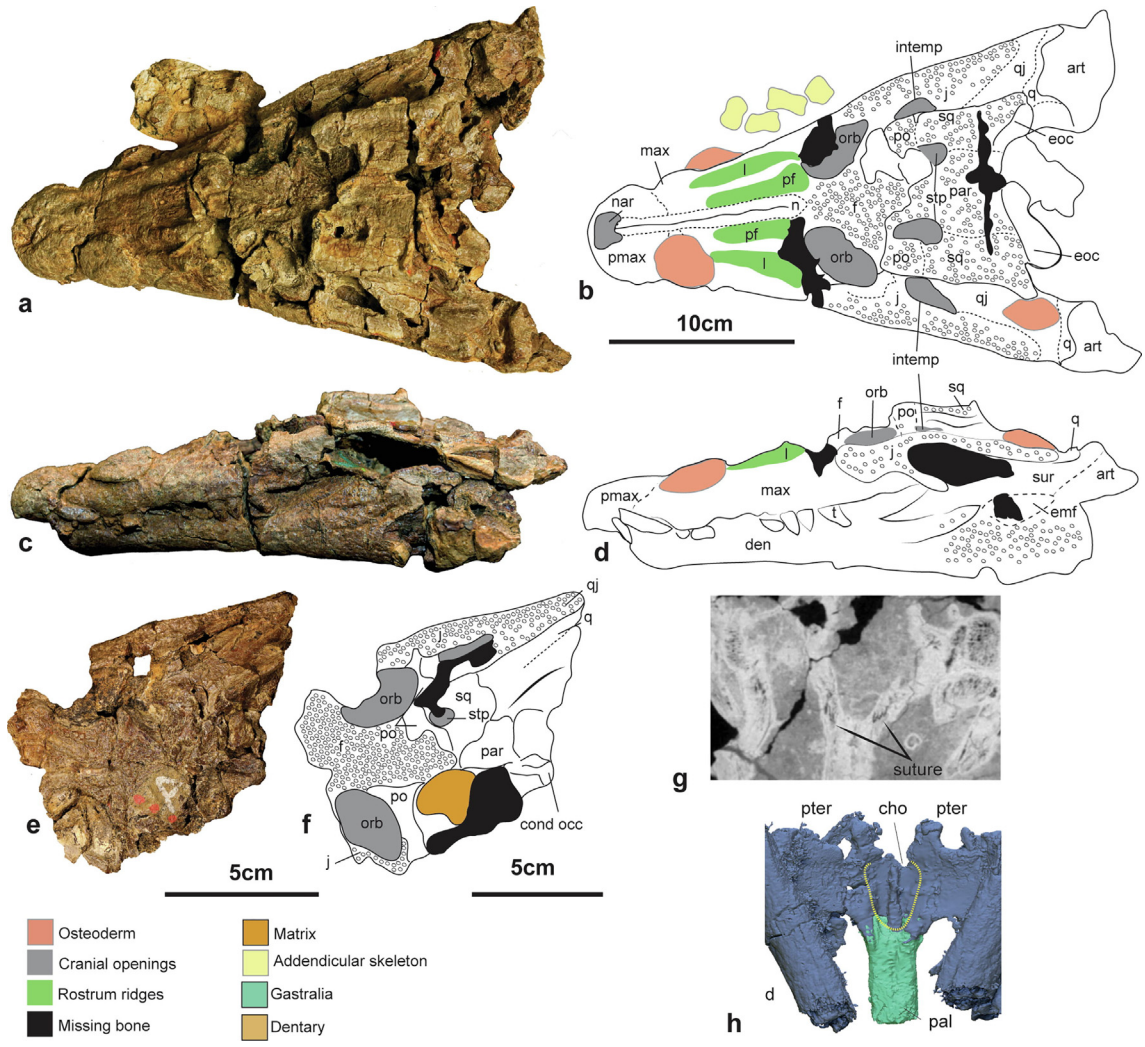

Fig. 2. Cranial and mandibular osteology of *Confractosuchus sauroktonos* gen. et sp. nov. (AODF0890). (a-b) dorsal view of skull; (c-d) left lateral view of skull; (e-f), dorsal view of posterior part of skull with skull table removed following a natural break; (g) synchrotron image of suture margins between the choana and palatines; (h) 3D render of the choana and palatine suture. Abbreviations: art, articular; cond occ, occipital condyle; cho, choana; den, dentary; eoc, exoccipital; emf, external mandibular fenestra; f, frontal; intemp, infratemporal fenestra; j, jugal; l, lacrimal; max, maxilla; n, nasal; nar, naris; orb, orbit; pal, palatine; par, parietal; pf, prefrontal; pmax, premaxilla; po, postorbital; pter, pterygoid; q, quadrate; qj, quadratojugal; s, scapula; sm, suture margins of cervical ribs; sq, squamosal; stp, superior temporal fossa; sur, surangular; t, tooth. Dotted lines represent suspected suture regions.

Martin et al. (2020)) and *Caiman crocodilus*, but distinct from the broad, platyrostral snout of susisuchids (Salisbury et al., 2006). Fusion or preservation (*via* ironstone replacement) masked the cranial sutures, and the majority of cranial bone contacts cannot be distinguished with certainty (Fig. 2; Supplementary Data, Figs. 2-4). The external narial opening is wider than long and partially invaded posteriorly by a blunt triangular projection of the paired nasals. The lateral edge of the oral margin is straight when viewed from the dorsal aspect, although the snout is medially pinched behind the naris, presumably to receive the enlarged fourth dentary tooth as in extant crocodylids. A relatively large dislodged tooth present in this region on the left side may be this tooth. Dorsally, the rostrum is ornamented by two pairs of anteroposteriorly-oriented longitudinal ridges that extend from the anterior margin of the orbit to a point in line with the fourth maxillary tooth. The medial ridge originates on the prefrontal, whereas the lateral ridge occupies the lacrimal; both ridges likely extend onto the maxilla, although fusion or preservation has obliterated most of the cranial sutures in this area. These ridges are similar to those possessed by some allogatorids including *Paleosuchus trigonatus* (see Fig. 8C in Brochu (1999)), *Alligator mississippiensis* (see Fig. 4C in Brochu (1999)), and *Melanosuchus niger* (see Fig. 7C & 61 in Brochu (1999)). The longitudinal rostral ridges of *Confractosuchus* are sub-parallel and anteriorly converging, like those of *A. mississippiensis,* but are distinctly more dorsally pronounced than in the latter species. The ridges are also pronounced in both *Melanosuchus* and *Paleosuchus*; however, the lateral ridges are anteriorly divergent, similar to *Caiman*, and unlike the convergent ridges of *Confractosuchus* (Fig. 5). Elsewhere, cranial ornamentation consists of shallow pits and grooves on the frontal, parietal, postorbital, squamosal, and lateral surface of the jugal and dentary. Ornamentation, aside from the longitudinal ridges, is not apparent on the rostrum (Fig. 2); however, ironstone may have masked such ornamentation, rendering comparisons problematic. The skull table (comprising the postorbitals, squamosals, and parietals) is roughly trapezoidal and concave posteriorly in dorsal aspect and appears devoid of a median crest like *Bernissartia* (see Fig. 4J in Martin et al. (2020)). The supratemporal fenestrae are small and oval, similar to but proportionally smaller than in *Bernissartia* (see Figs. 1-3 in Martin et al. (2020)). The dorsolaterally-facing infratemporal fenestra is teardrop-shaped and attenuates caudolaterally. The postorbital bar is poorly preserved and its overall morphology could not be distinguished. From contact with the postorbitals, the frontal converges rostromedially before diverging again to a

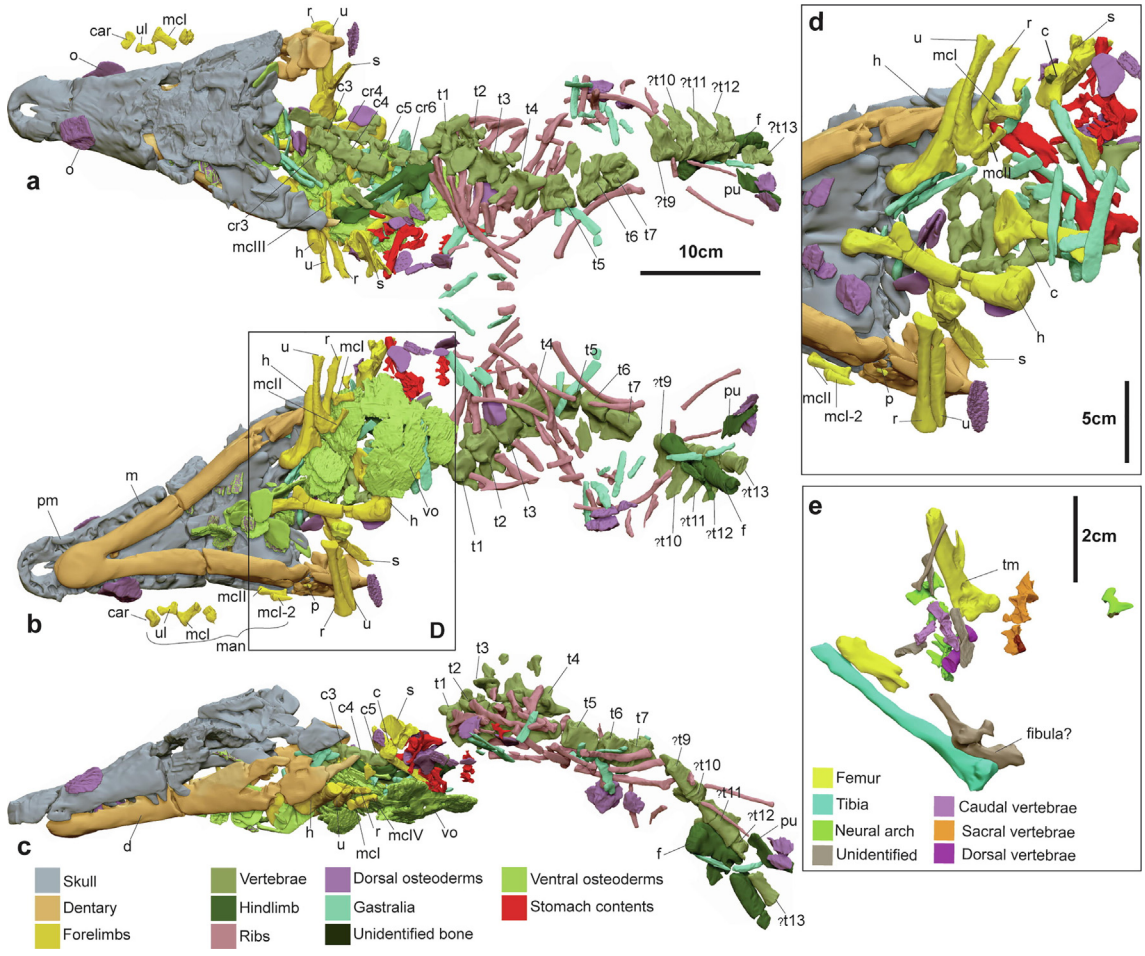

Fig. 3. Digital dissection of *Confractosuchus sauroktonos* gen. et sp. nov (AODF0890) in (a) dorsal aspect; (c) ventral aspect; (c) left lateral aspect; (d) close-up of pectoral region with ventral osteoderms removed (in ventral aspect); (e) abdominal contents showing ornithopod remains. Abbreviations: c, coracoid; car, carpal; c(no.), cervical vertebrae (number); cho, choana; cr3, cervical rib 3; d, dentary; f, femur; h, humerus; mcI, metacarpal 1; mc1-1, manual phalanx 1–1; mcI-2, manual phalanx I-2; mcII metacarpal 2; mcIII metacarpal III; mcV metacarpal 5; man, manus; o, osteoderm; p, manual phalanx; pal, palatines; pter, pterygoids; pu, pubis; r, radius; s, scapula; tm, tooth mark; t(no.), thoracic vertebrae (number); u, ulna; ul, ulnare; vo, ventral osteoderm.

lesser degree more rostrally, defining the dorsal margin of the elliptical orbits (Fig. 2). Unlike *Susisuchus* and *Isisfordia*, there is no defined supraorbital ridge on the frontal. Both jugals are damaged; however, they clearly form the lateral margins of the orbits and the intertemporal fenestrae. Like *Susisuchus* and *Isisfordia,* the jugal is arched beneath the orbits but flattens when bordering the intertemporal fenestrae. The exoccipital region is poorly preserved masking the supraoccipital and the posterior end of the parietals. Despite this, an exposed portion reveals that the exoccipital is smooth. All other parts of the braincase are obscured by matrix.

Imaging and medical beamline (100 μm) revealed a secondary palate with an anteriorly positioned choana, bound anteriorly by the palatines and divided by a median septum (Fig. 2GH) like *Bernissartia* (see Figs. 2 and 3 in Martin et al. 2020). The anterior edge of the choana is situated anterior to the posterior edge of the suborbital fenestra, a characteristic shared with *Isisfordia* (see Fig. 4 in Salisbury et al. 2006). The width of the choana is similar to the minimum mediolateral width of the palatine (Fig. 2GH). These characteristics combined appear to be unique for *Confractosuchus*; however, this claim is weak given the poor preservation and/or figuring of comparable specimens.

The occipital surface of the basicranium and basisphenoid ventral to the occipital condyle is currently covered in matrix and requires preparation to reveal its morphological features; it was not clear in the synchrotron images. In lateral aspect, the postorbital-squamosal forms a lateral shelf overhanging the incisura otica, which is only visible on the left side of the skull. The shelf is ventrally convex with a longitudinal groove bisecting it centrally, which is mostly formed by the squamosal.

Both mandibular rami are preserved in tight occlusion with the upper jaws; however, individual sutures delineating the dentary, splenial, surangular, and angular are indistinct. Grooves in this region may in fact identify the suture margins (Fig. 2D). The occlusal margin of the dentary is straight and the external mandibular fenestra is semicircular (height:length ≈ 1) (flat ventrally) unlike the elongate opening in *Isisfordia* and Crocodylia (Salisbury et al., 2006). Ornamentation is restricted to the posterior one-quarter of the mandible and likely did not extend onto the dentary. There are 4 premaxillary, 12 maxillary and 17 dentary teeth (revealed by imaging and medical beamline) that occlude in an overbite pattern. The teeth are conical and homodont with weak mesial and distal carinae, which is unlike the robust hypertrophied teeth of hylaeochampsids (Boyd, Drumheller and Gates, 2013; Narváez et al., 2015) or the small, labiolingually flattened teeth of susisuchids that become conical apically (Salisbury et al., 2006).

3.8.2. Vertebrae

The vertebral column is incomplete, consisting of cervicals c3–5 and thoracics t1–7, t?9–13. Interestingly the vertebral form is

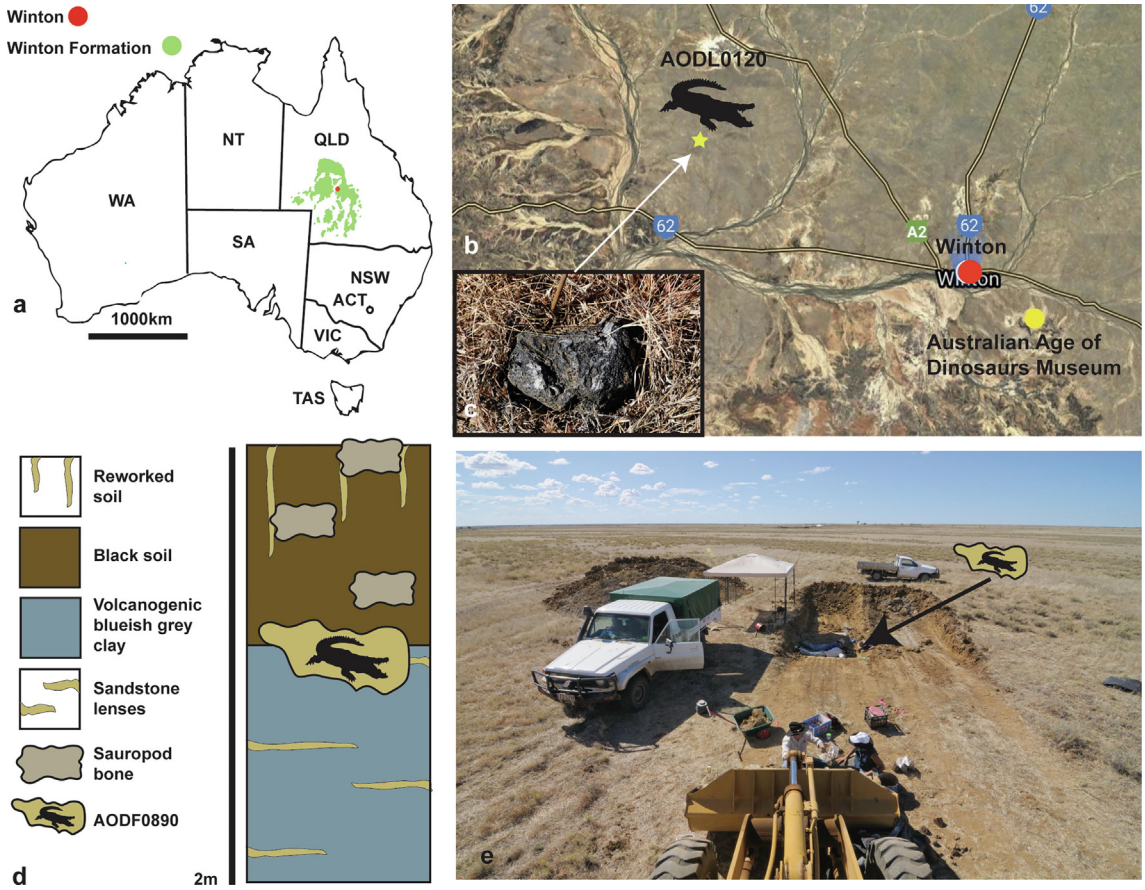

Fig. 4. Australian Age of Dinosaurs Locality 0120. (a) schematic of modern-day Australia with the Winton Formation (in green) and the position of Winton (red dot); (b) satellite image of locality in relation to the town of Winton and the Australian Age of Dinosaurs Museum; (c) image of sauropod bone found *in situ* at the surface; (d) stratigraphy of AODL0120; (e) photograph of AODL 0120.

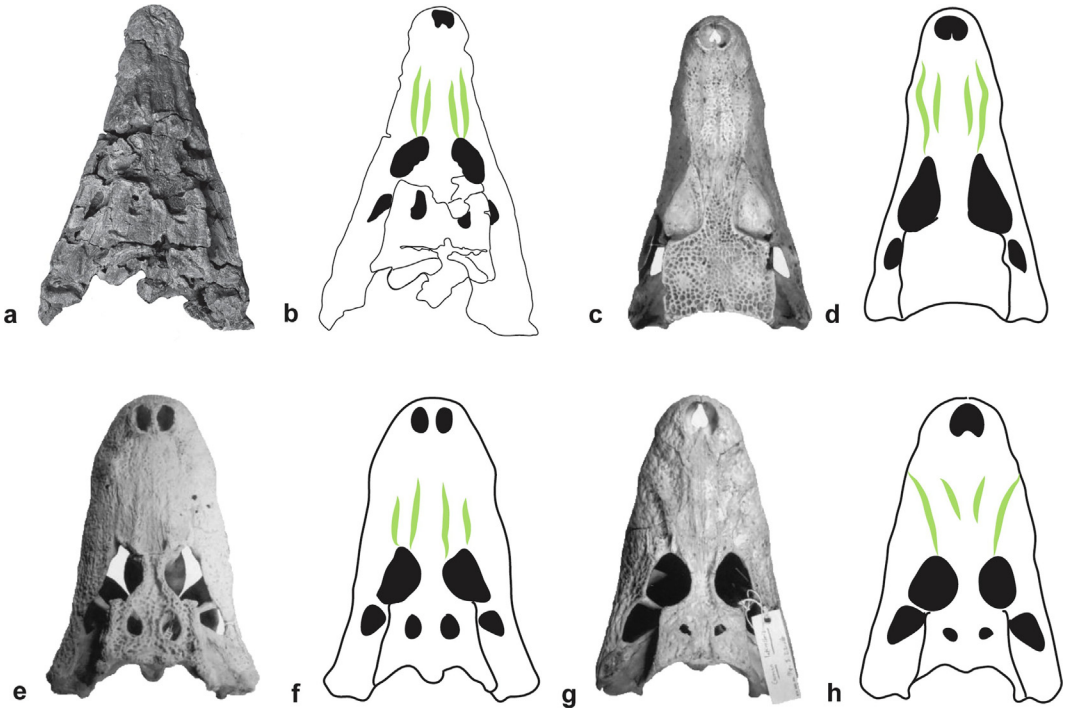

Fig. 5. Examples of extant alligatoroid skulls with rostral ridges compared with *Confractosuchus*. (a-b) *Confractosuchus sauroktonos* gen. et sp. nov; (c-d) *Paleosuchus palpebrosus* (obtained from Fig. 8 in Brochu (1999); (e-f) *Alligator mississippiensis* (United States National Museum (USNM) 292078) (modified from Fig. 4 in Brochu (1999); G-H, *Caiman latirostris* (modified from Fig. 7 in Brochu (1999)).

strongly regionalised, revealed via segmentation of the synchrotron data (see diagnosis). The centra and corresponding neural arches are fused in the thoracic vertebrae but are open in the cervical series, indicating the individual was sub-adult at the time of death (Brochu, 1996) (Fig. 3A and Fig. 6; Supplementary Data, Fig. S5).

3.8.3. Cervical vertebrae

There are three preserved cervical vertebrae in articulation, which we identify as C3-5. The neural arches are missing along the neurocentral suture indicating that fusion with the vertebral centra had not yet occurred. The centra have an incipiently procoelous condition in which the anterior surface is shallowly concave and the posterior condyle is shallowly convex with a small depression in its centre, like that described in *Theriosuchus* (Salisbury and Frey, 2001), *Pachycheilosuchus* (Rogers, 2003) and *Isisfordia* cf. *I. selaslophensis* (Hart et al., 2021). A weekly developed keel is present on c4 and c5 (Fig. 7; Supplementary Data, Fig. S6).

3.8.4. Thoracic vertebrae

Twelve partial and complete thoracic vertebrae are preserved consisting of t1–7, and t9?–13? (Figs. 8-9; Supplementary Data, Fig. S7-8). All thoracic vertebrae have closed neurocentral sutures, although the neural arches of t5–9 are broken and largely missing. Thoracic vertebrae t1 and t2 are procoelous, t3 is incipiently procoelous whereas t4–9 are amphicoelous, t10 appears weakly procoelous, t11–13 amphicoelous. This varying thoracic condition has been inadvertently referred to as occurring in some neosuchians such as *Theriosuchus*, which is said to have "at least some procoelous vertebrae" (Turner, 2015), and *Shamosuchus* where the cervical and first dorsal vertebra was noted as being procoelous (Turner, 2015). The allodaposuchids *Allodaposuchus hulki* (Blanco et al. 2015), *Allodaposuchus palustris* (Blanco et al. 2014), *Allodaposuchus precedens* (Narváez et al. 2020) were all described as possessing strongly procoelous vertebra with no mention of varying morphology. Vertebral morphology varies between members of Susisuchidae: *Isisfordia duncani* was described as a transitional form with the presence of incipiently procoelous vertebrae, whereas *Susisuchus* appears to possess only amphicoelous vertebrae (see Fig. 5 in Salisbury et al. 2006). Susisuchidae is typically regarded as phylogenetically near Eusuchia; however, its exact placement remains uncertain (Salisbury et al. 2006; Turner and Pritchard 2015). The varying vertebral morphology possessed by *Confractosuchus* alludes to a transitional morphology, and also supports a phylogenetic position near Eusuchia.

The first three thoracic vertebrae have a pronounced hypapophysis which tapers posteriorly into a ventral keel. A less pronounced hypapophysis is preserved on t4, which has a correspondingly reduced ventral keel. Both features are non-existent in t5–13. The anterior thoracic vertebrae t1–4 have constricted (hourglass-shaped) centra, whereas the centra of t5–13 are more cylindrical. Centra increase in length from the first thoracic vertebra. The

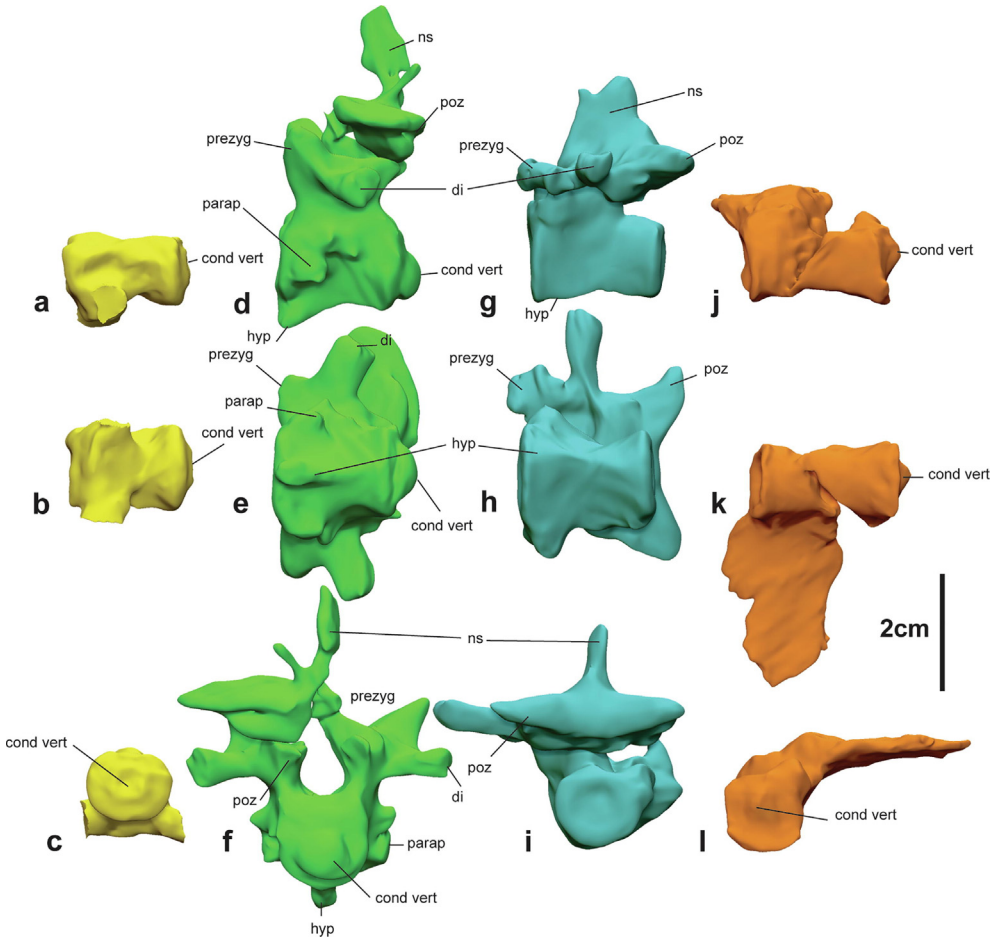

Fig. 6. Various vertebrae morphologies identified in *Confractosuchus sauroktonos* gen. et sp. nov. Vertebrae in: left lateral (a, d, g, j); ventral (b, e, h, k); and posterior (c, f, i, l) views. (a-c) cervical vertebra 5 with incipiently procoelous condition; (d-f) thoracic vertebra 2 with procoelous condition; (g-i), thoracic vertebrae 3 with amphicoelous condition; (j-l), thoracic vertebrae 10 with slight incipient condition. Abbreviations: prezyg, prezygapophysis; cond vert, vertebral condyle; di, diapophysis; hyp, hypapophysis; ns, neural spine; parap, parapophysis; poz, postzygapophysis.

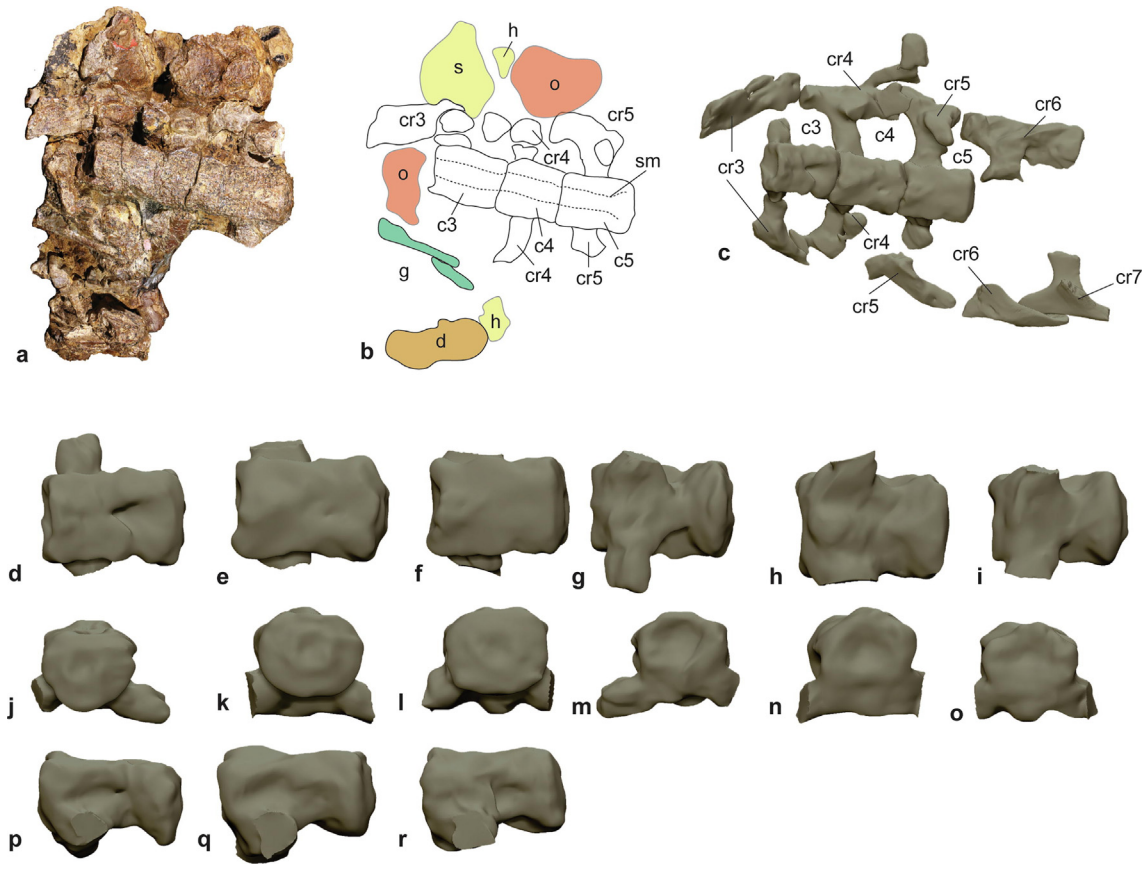

Fig. 7. *Confractosuchus sauroktonos* gen. et sp. nov. cervical vertebrae and associated elements. (a) photograph; (b) 2D schematic of elements in dorsal view; (c) 3D representation of the cervical vertebrae in dorsal aspect with associated cervical ribs (other elements removed). Digital renders of individual cervical vertebrae in dorsal aspect (d, c3; e, c4; f, c5); ventral aspect (g, c3; h, c4; I, c5); posterior aspect (j, c3; k, c4; l, c5); anterior aspect (m, c3; n, c4; o, c5); left lateral aspect (p, c3; q, c4; r, c5). Abbreviations: c, cervical vertebrae; cr, cervical rib; d, dentary; g, gastralia; h, humerus; o, osteoderm.

parapophysis is situated mid-height on the anterior margin of t1-2 and becomes less pronounced on the more posterior centra. Pre- and postzygapophyses and both the diapophysis and parapophysis are too poorly preserved and/or digitally represented to warrant detailed descriptions. The first four vertebrae articulate or are near enough associated with their corresponding ribs, confirming that the first four ribs have a distinct branch separating the capitulum and tuberculum. Posterior of the fourth vertebra, the preservation and digital resolution deteriorates due to ironstone; however, the few disarticulated ribs that are preserved in close proximity to t7 and t9 have no distinct branching of the capitulum and tuberculum and indicate a shift towards aligning in the same plane as is the case in living crocodiles.

3.8.5. Scapula

Both scapulae are preserved. The right scapula is more complete than the left, preserving some of the blade and near complete acromion process, scapular synchondrosis and glenoid fossa. The left is represented by an incomplete scapular synchrondrosis. The blade is only partially preserved but an antero-posterior constriction is apparent. In lateral view, the scapular blade is oblique to the synchrondrosis for the coracoid. A shallow curved deltoid crest is visible is both anterior and medial views. Lateral to the deltoid crest, in anterior aspect, the acromion process forms a dorsal lip over the scapular synchondrosis (Fig. 10; Supplementary Data Fig. S9-10).

3.8.6. Coracoids

Both coracoids are near complete with the left missing a small portion of the articular surface that articulated with the scapula synchondrosis (coracoid contact surface). It has a pendulous contribution to the glenoid facet on its posterior side. The long ventral shaft is medially bowed, constricted at the midpoint and becomes fan-shaped distally (in mediolateral views) with a convex termination. In medial and lateral views, the blade is almost symmetrical. The proximal anterior edge has a pointed process. The coracoid foramen is circular. The coracoid forms more of the glenoid facet than the scapula. The sutural surface with the scapula slopes proximally but is slightly convex (Fig. 11; Supplementary Data, Fig. S11-12).

3.8.7. Shoulder girdle

The shoulder girdle of *Confractosuchus* closely resembles *Anteophthalmosuchus hooleyi* (see Fig. 16 in (Martin Delfino and Smith, 2016)). *Anteophthalmosuchus* shoulder girdle morphology was reported to be similar to *Isisfordia duncani* (scapula only see Fig. 2 in Salisbury et al. (2006) and *Susisuchus anatoceps* (schematic outline, see Fig. 3 in Salisbury et al. (2003); however, the published images of both these susisuchids were insufficient to draw such similarities to *Confractosuchus*. A resemblance with *Pachycheilosuchus trinquei* (Rogers, 2003) can be established despite a slightly different orientation in the figures and only one view supplied of each (see Fig. 6A,B in Rogers (2003)). Much like the description of *Anteophthalmosuchus hooleyi* (Martin, Delfino and Smith, 2016) the coracoid resembles the morphology of eusuchians.

3.8.8. Forelimb

The forelimbs are mostly adducted beneath the chest cavity and most of the elements have shifted from life position but remain on

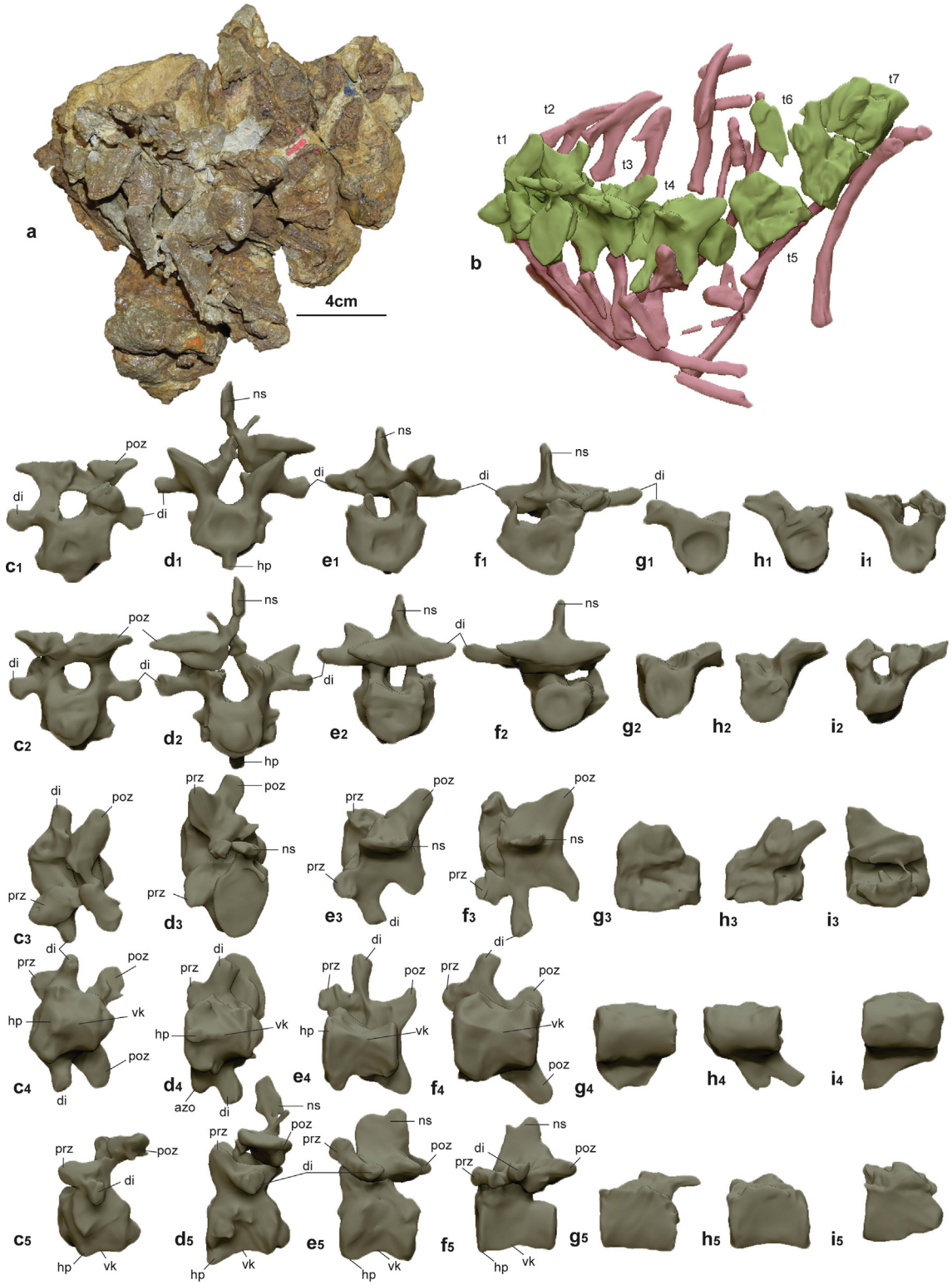

Fig. 8. Thoracic elements of *Confractosuchus sauroktonos* gen. et sp. nov. in (a), block containing thoracic vertebrae t1-7 and associated thoracic ribs in dorsal aspect; (b), 3D schematic of elements in (a); (c1-5) thoracic vertebra 1; (d1-5) thoracic vertebra 2; (e1-5) thoracic vertebra 3; (f1-5) thoracic vertebra 4; (g1-5) thoracic vertebra 5; (h1-5) thoracic vertebra 6; (i1-5) thoracic vertebra 7; (c1, d1, e1, f1, g1, h1) in anterior aspect; (c2, d2, e2, f2, g2, h2, i2) posterior aspect; (c3, d3, e3, f3, g3, h3, i3) dorsal aspect; (c4, d4, e4, f4, g4, h4, i4) ventral aspect; (c5, d5, e5, f5, g5, h5, i5) lateral aspect. Abbreviations: prz, prezygapophysis; di, diapophysis; hp, hypapophysis; ns, neural spine; poz, postzygapophysis; t, thoracic vertebrae; vk, ventral keel.

their respective sides. Of these forelimb elements, the right ulna and radius are the only ones that appear to be articulated. The right manus is disarticulated on the right-hand side of the rostrum whereas elements of the left manus are randomly dispersed around the left shoulder girdle (Fig. 3 and Supplementary Data, Fig. S4).

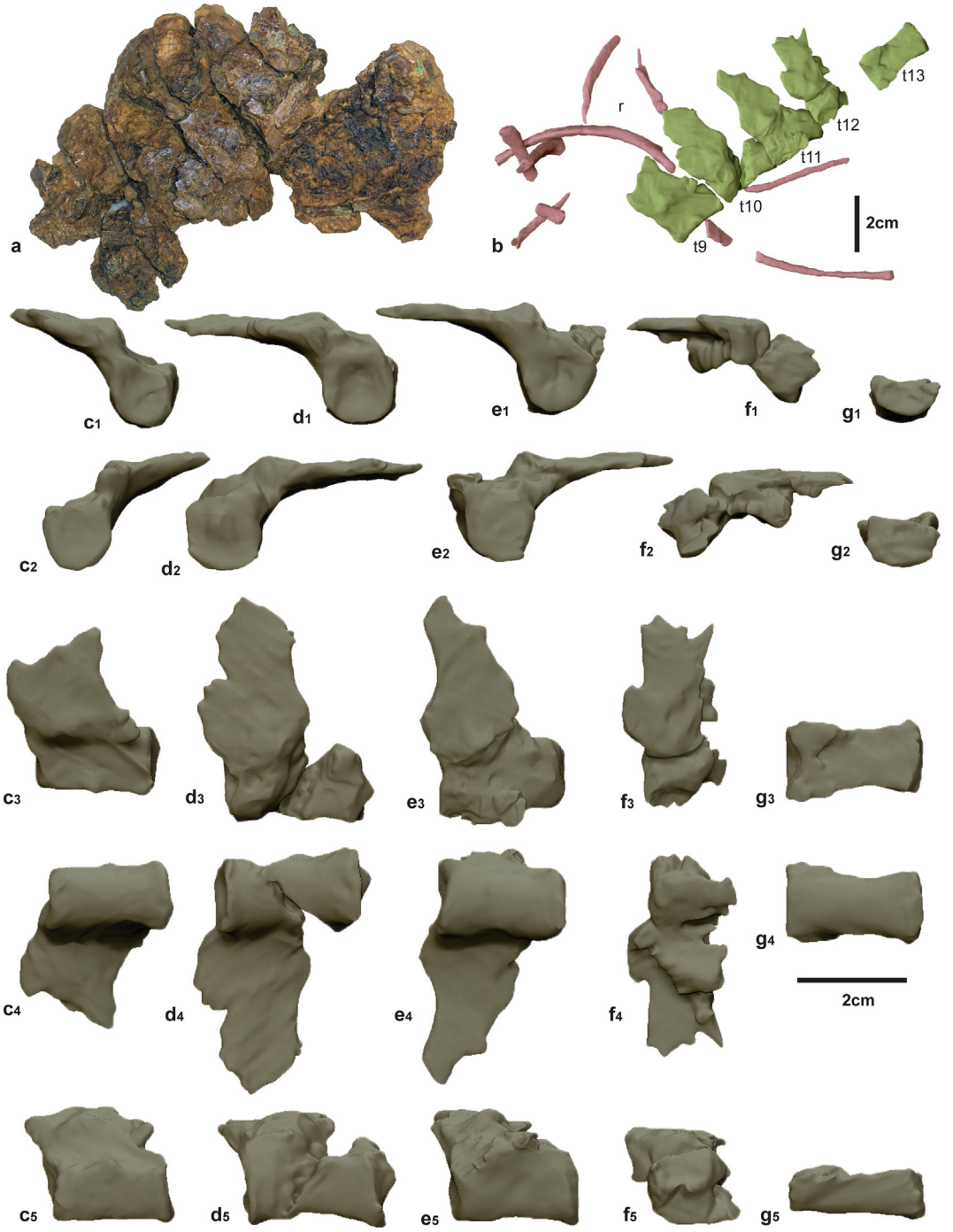

Fig. 9. Thoracic elements of *Confractosuchus sauroktonos* gen. et sp. nov. (a), block containing thoracic vertebrae t9-13 and associated thoracic ribs in dorsal aspect; (b) 3D schematic of elements in (a); (c1-5) thoracic vertebra 9; (d1-5) thoracic vertebra 10; (e1-5) thoracic vertebra 11; (f1-5) thoracic vertebra 12; (g1-5) thoracic vertebra 13; (c1, d1, e1, f1, g1) in anterior aspect; (c2, d2, e2, f2, g2) in posterior aspect; (c3, d3, e3, f3, g3) in dorsal aspect; (c4, d4, e4, f4, g4) in ventral aspect; (c5, d5, e5, f5, g5) in lateral aspect. Abbreviations: t, thoracic vertebrae; r, rib.

3.8.9. Humerus

The right humerus is complete (10.1 cm long) whereas the left is missing the distal end. In anterior and posterior aspects, the shaft is straight whereas in medial and lateral views the shaft is sigmoidal. The proximal head of the humerus is slightly offset from the shaft. It is convex dorsally, expanded transversely and inclined slightly medially. In dorsal aspect, the medial head is anteroposteriorly thicker than the lateral head. In lateral aspect, the deltopectoral crest is well developed with its proximal margin flat, rounding at its anterior margin forming a tuberosity that tapers distally, merging with shaft within the proximal half of the element. In anterior aspect, the deltopectoral crest is offset medially. In posterior aspect, the ulnar hemicondyle is marginally longer than the radial hemicondyle. A deep depression occupies the distal third of the posterior ulna surface, which in distal aspect separates the medial and lateral malleoli as a shallow groove (Fig. 12; Supplementary Data, Fig. S13-14).

3.8.10. Ulnae

Both ulnae are partially preserved but together permit the description of the entire element (estimated length ~ 7.5 cm). The proximal portion of the ulna shaft is strongly bowed relative

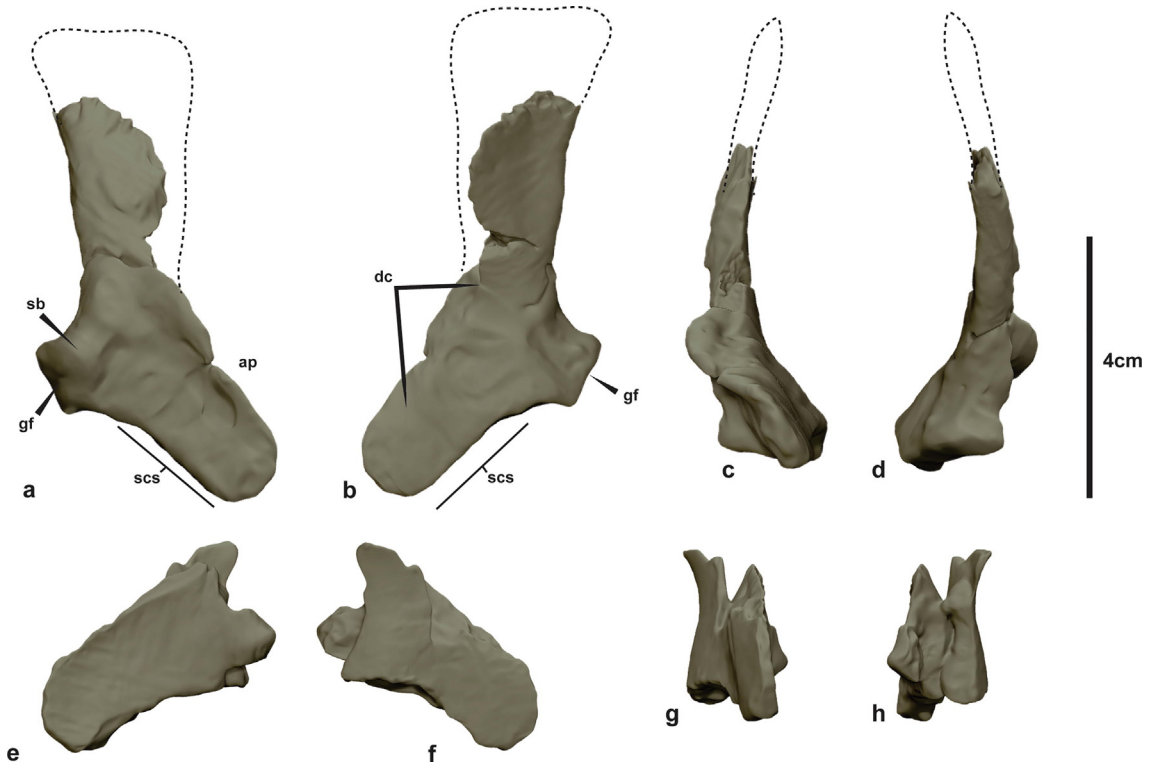

Fig. 10. Digital renders of the scapulae of *Confractosuchus sauroktonos* gen. et sp. nov. Right scapula in: (a) lateral; (b) medial; (c) anterior; (d) posterior. Left scapula in: (e) lateral; (f) medial; (g) anterior; (h) posterior. Abbreviations: ap, acromion process; dc, deltoid crest; gf, glenoid fossa; sb, supraglenoid buttress; scs, scapula synchondrosis.

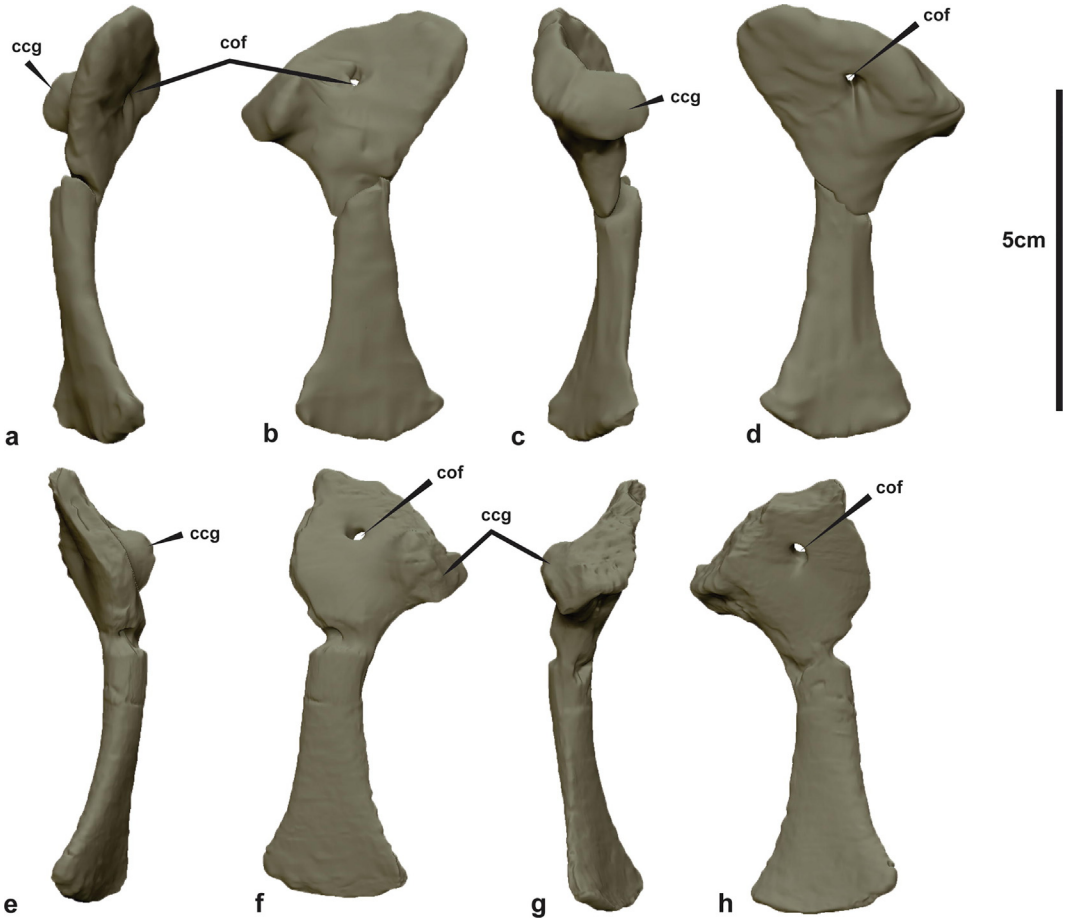

Fig. 11. Digital renders of the coracoids of *Confractosuchus sauroktonos* gen. et sp. nov. Right coracoid in: (a) anterior; (b) lateral; (c) posterior; (d) medial. Left coracoid in: (e) anterior; (f) lateral; (g) posterior; (h) medial. Abbreviations: ccg, coracoid contribution to glenoid; cof, coracoid foramen.

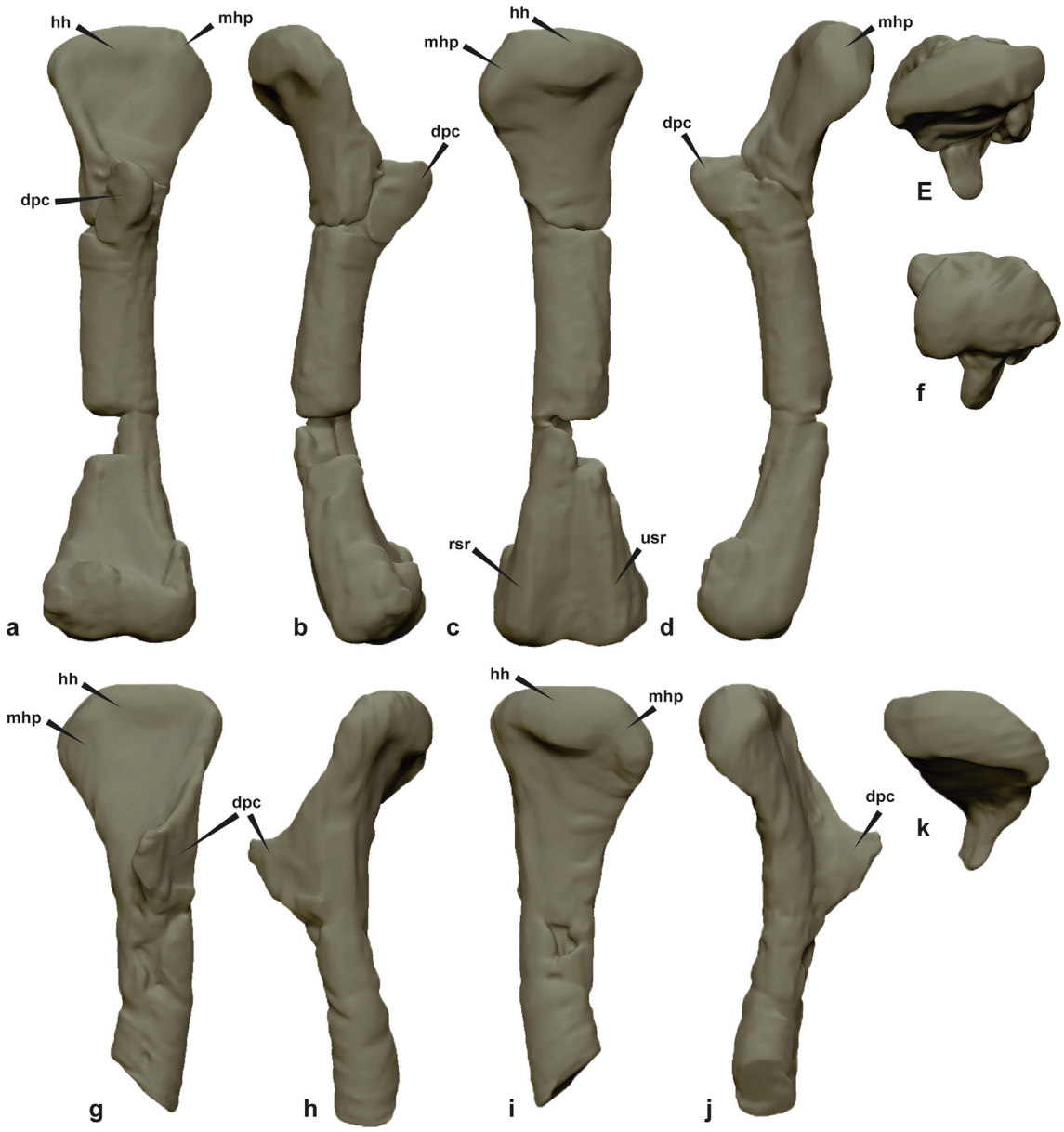

Fig. 12. Digital renders of the right and left humerus of *Confractosuchus sauroktonos* gen. et sp. nov. Right humerus in: (a) anterior; (b) lateral; (c) posterior; (d) medial; (e) proximal; (f) distal. Left humerus in: (g) anterior; (h) lateral; (i) posterior; (j) medial; (k) proximal. Abbreviations: dpc, deltopectoral crest; hh, humeral head; mhp, medial humeral process; rsr, radial supracondylar ridge; usr, ulnar supracondylar ridge.

to the main shaft in lateral aspect. The proximal end of the ulna is sub-circular in proximal view and expanded relative to the shaft, with an undulating proximal surface: the olecranon process is indistinguishable. In anterior aspect, the proximal head of the ulna overhangs the radial facet. The shaft is ovoid in cross-section becoming mediolaterally compressed and anteroposteriorly expanded at its distal end (Fig. 13; Supplementary Data, Fig. S15-16).

3.8.11. Radii

Both radii are preserved. The right is complete (6.7 cm long) whereas the left is missing the distal one-quarter. The proximal end is mediolaterally and, to a lesser extent, anteroposteriorly expanded relative to the shaft. The proximal articular surface itself is concave and ovoid in proximal view. The shaft is straight, elliptical in cross-section, flaring mediolaterally at the distal end. The distal articular surface is flat (Fig. 14; Supplementary Data, Fig. S17-18).

3.8.12. Ulnare

The ulnare is hourglass-shaped, and strongly expanded mediolaterally at both the proximal and distal ends. The proximal end is hemispherical, whereas in anterior view, the distal end is boot-shaped, projecting from the shaft more on the lateral margin. A concavity on the distomedial margin is likely the facet for the radiale. In distal aspect, the terminus is flat and tear-drop shaped, tapering laterally (Fig. 15A-D; Supplementary Data, Fig. S19).

3.8.13. Manus

The manus elements of *Confractosuchus* were identified by comparing them with *Crocodylus porosus*. These comparisons were completed digitally using scans of *Crocodylus porosus* that were initially used to analyse limb musculature (Klinkhamer et al., 2017).

Eight elements of the right manus and five elements from the left have been preserved including: left and right metacarpals I and II (Supplementary Data, Figs. S20-23), left metacarpal III (Supplementary Data, Fig. S24), right metacarpal IV (?) (Supplementary

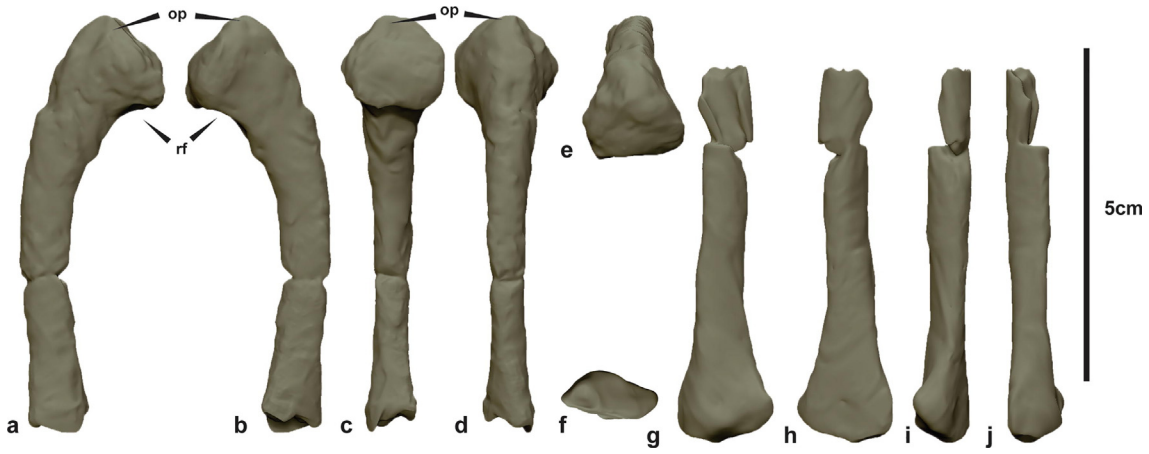

Fig. 13. Digital renders of the left and right ulna of *Confractosuchus sauroktonos* gen. et sp. nov. Left ulna in: (a) medial; (b) lateral; (c) anterior; (d) posterior; (e) proximal; (f) distal. Right ulna in: (g) lateral; (h) medial; (i) anterior; (j) posterior. Abbreviations: op, olecranon process; rf, radial facet.

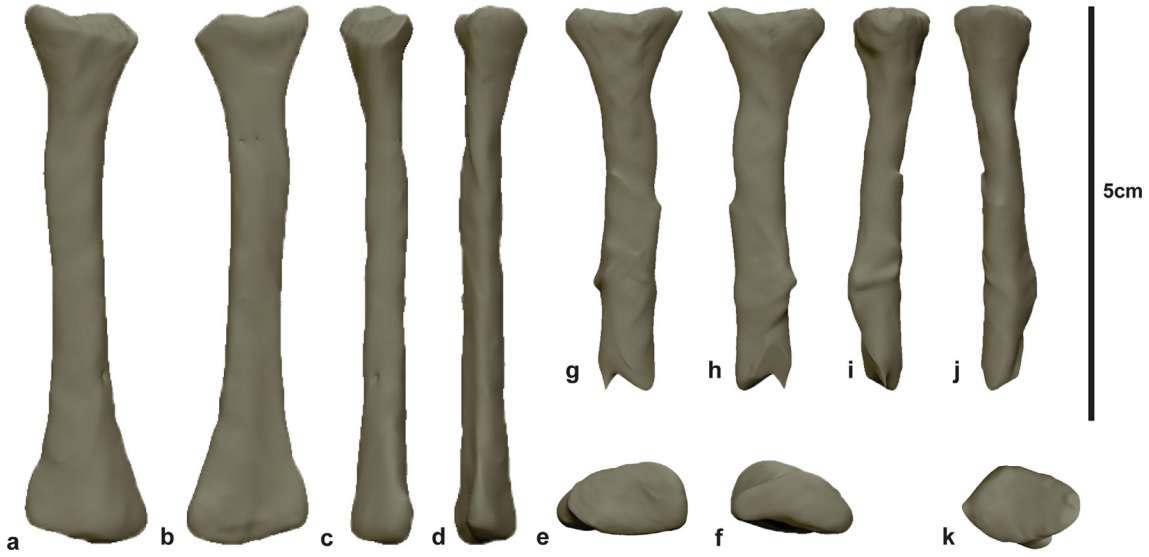

Fig. 14. Digital renders of the left and right radius of *Confractosuchus sauroktonos* gen. et sp. nov. Right radius in: (a) anterior; (b) posterior; (c) medial; (d) lateral; (e) proximal; (f),distal. Left radius in: (g) posterior; (h) anterior; (i) medial; (j) lateral; (k) proximal.

Data, Fig. S25), with two suspected adjoining phalanges IV-1 and IV-2; a right ungual I-2 (Supplementary Data, Fig. S26) and a suspected left phalanx IV-2 (Fig. 15).

Metacarpal I is robust with an expanded proximal end and a weakly expanded distal end. In proximal aspect it is tear-drop shaped, tapering laterally. A small circular facet on the proximolateral surface forms the articulation with metacarpal II. In distal aspect it appears rectangular with the lateral condyle slightly taller than the medial. The shaft is more concave on its lateral side and is dorsoventrally flattened. It is the broadest of the metacarpals.

Metacarpal II is longer and more gracile than metacarpal I. It is slightly fan shaped at the proximal end with a medial projection to receive metatarsal I. In proximal aspect it is ovoid with the anterior margin slightly concave. In distal aspect the end is rectangular with the anterior margin slightly concave. In relation to the proximal end, the distal end is rotated ~ 45° clockwise. The shaft is mostly circular in cross section.

Metacarpal III is the longest and most gracile of the metacarpals (Fig. 15). In anterior aspect the proximal end is fan-shaped with a shallow circular region on its medial margin to receive metacarpal II. In proximal aspect it is ovoid with a slightly concave posterior margin. In distal aspect it is rectangular and, like metacarpal II, the distal end is rotated clockwise in relation to the proximal end, but to a less extent (~30°). The shaft is mostly circular in cross section.

Metacarpal IV (?) is the smallest of the recovered metacarpals. In both proximal and distal aspects, it is ovoid. The shaft is circular in cross section.

3.8.14. Pelvic girdle

The only element that is preserved of the pelvic girdle is the distal part of the left pubis. The remaining part of the shaft close to the distal end is ovoid in cross-section. The distal blade is spatulate with a wing-shaped, triangular lateral margin, whereas the medial margin missing (Fig. 16, Supplementary Data, Fig. S27).

3.8.15. Femur

The only element of the hindlimb that was recovered is a partial right femur, which is broken in two below the level of the fourth trochanter. The distal one-third of the femur is also missing; however, enough of it is preserved to indicate the shaft was sigmoid in lateral view. In proximal aspect the lateral margin is flat whereas

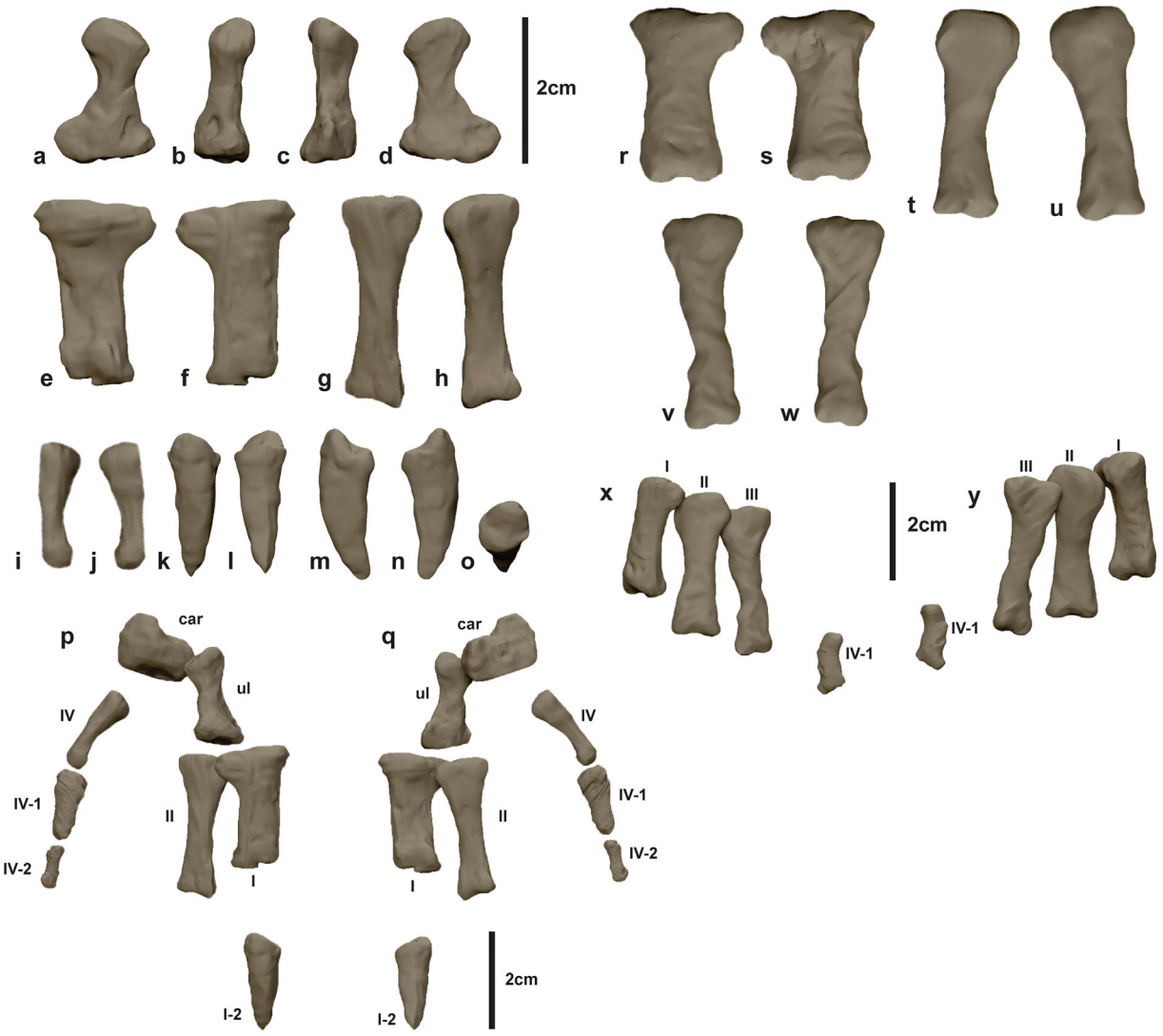

Fig. 15. Digital renders of the manual elements of *Confractosuchus sauroktonos* gen. et sp. nov. (a-q) Right manus. (r-y) Left manus. Right manus. Ulnare in: (a) anterior, (b) medial, (c) lateral, (d) posterior views. Metacarpal I in: (e) anterior, (f) posterior views. Metacarpal II in: (g) anterior, (h) posterior aspect. Metacarpal IV(?) in: (i) anterior, (j) posterior. Manual phalanx I-2 in: (k) anterior, (l) posterior, (m) medial, (n) lateral, (o) proximal views. Right manus in: (p), anterior; (q), posterior views. Left manus. Metacarpal I in: (r) anterior, (s) posterior views. Metacarpal II in: (t) anterior, (u) posterior views. Metacarpal III in: (v) anterior, (w) posterior views. Left manus in: (x) anterior, (y) posterior views. Abbreviations: car, carpal; ul, ulnare.

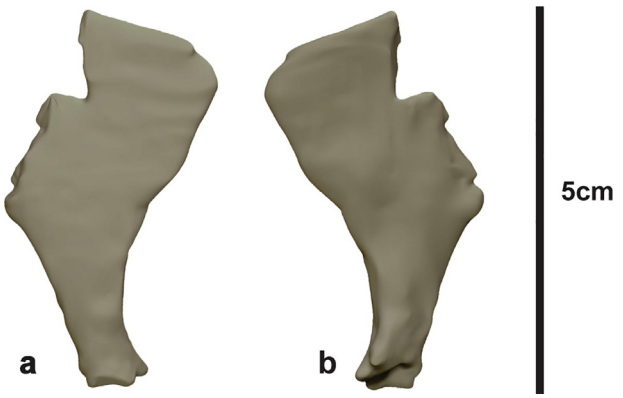

Fig. 16. Left pubis of *Confractosuchus sauroktonos* gen. et sp. nov. Left pubis in: (a) dorsal; (b) ventral view.

the medial margin bears a proximal tuberosity with a notable protuberance. The fourth trochanter is a broad, rounded ridge; however, it is poorly preserved and incomplete due to a transverse break (diagenetic origin) in this region. More distally, the remaining part of the shaft is circular in cross-section (Fig. 17; Supplementary Data, Fig. S28).

3.8.16. Osteoderms

The dermal armour is entirely disarticulated. Osteoderms evidently lack an anterior articulating process and, when complete, are mostly ovoid. They are deeply pitted with a central ridge or keel (Fig. 18); however; none of them are biserial (larger, twin-keeled), supporting the interpretation of an entirely segmented paravertebral shield as in *Susisuchus* and *Isisfordia* (Salisbury et al., 2006; Figueiredo et al., 2011) but unlike *Bernissartia* (Salisbury et al., 2006; Buscalioni and Sanz, 1990) (Supplementary Data, Fig. S29). Un-keeled, mostly circular, pitted osteoderms clustered on the ventral part of the neck probably formed part of the displaced gastral shield (Fig. 3B; Supplementary Data, Fig. S30). The fully segmented paravertebral shield, enabled greater lateral and dorso-ventral flexion of the trunk, an adaptation for improved aquatic locomotion (Salisbury and Frey, 2001; Molnar et al., 2015). Larger, more primitive crocodyliforms such as goniopholids and

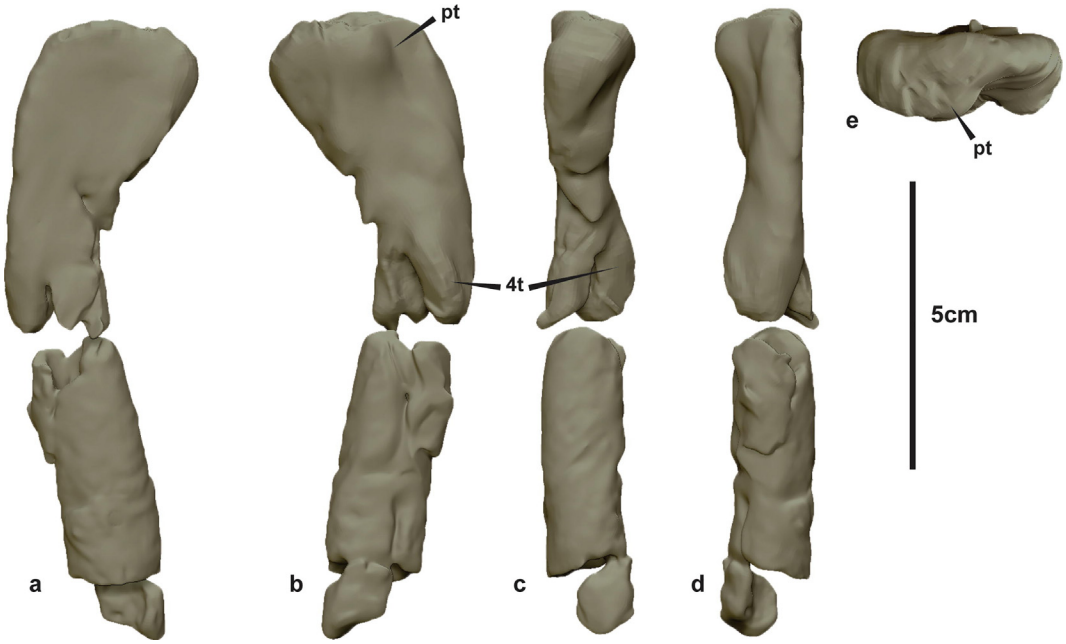

Fig. 17. Right femur of *Confractosuchus sauroktonos* gen. et sp. nov. Femur in: (a) anterior; (b) medial; (c) posterior; (d) lateral views. Abbreviation: pt, proximal tuberosity; 4 t, fourth trochanter.

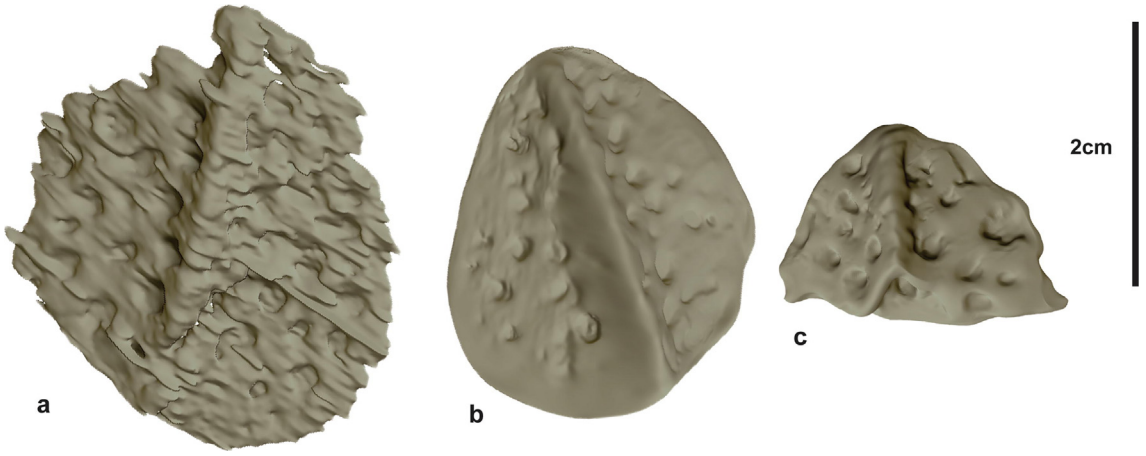

Fig. 18. Dorsal osteoderms of *Confractosuchus sauroktonos* gen. et sp. nov. (a-c), individual osteoderms. A, scanned at 100 μm; B-C, scanned at 15 μm.

pholidosaurids that possessed amphicoelous vertebrae, were cloaked in a closed, interlocking paravertebral shield that enabled sustained terrestrial walking regardless of size (Salisbury and Frey, 2001; Molnar et al., 2015); however, they lacked lateral and dorsoventral flexion of more derived crocodyliforms.

3.9. Abdominal contents

Collectively, the ornithopod remains comprise three dorsal vertebrae, two sacral centra, three distal caudal centra, both proximal femora, left tibia, and several other elements that could not be identified from the synchrotron data, all presumably from a single individual (based on their relative size and non-repeating elements) (Supplementary Data, Figs. S31-34). Successive vertebrae in each of the three main regions (dorsal, sacral, caudal) are articulated-to-associated, although these regions are non-contiguous (e.g. articulated sacral vertebrae are not continuous with the articulated caudal vertebrae), suggesting connective tissues were still intact at the time its consumer died. The two articulated dorsal centra are spool-shaped, amphiplatyan, and unfused to their respective neural arches. A second string of three semi-articulated vertebra all lack their neural arches. Comparisons with other more complete vertebral series (Galton, 1974; Salgado, Coria and Heredia, 1997; Scheetz, 1999) indicate that these represent the last dorsal and first two sacral centra. The sacral centra are dorsoventrally low, amphiplatyan, and strongly mediolaterally expanded at both anterior and posterior ends forming prominent sacral rib attachments. The sacral ribs themselves are not preserved. The three caudal centra are articulated and likely derive from the distal part of the series based on anteroposteriorly elongate proportions and absence of transverse processes. No caudal neural arches are present on any of the caudal vertebrae. The lack of fusion between the dorsal centra and their neural arches and between the sacral centra (Galton, 1974), together with the overall small size of the specimen, suggest a juvenile status.

Both femora are incomplete, sheared obliquely below the level of the fourth trochanter, the right presumably as a result of oral processing, whereas the left was the result of excavation. Despite

breakage, the femur is bowed in lateral view and the pendant fourth trochanter would have been located within the proximal half of the element, as is typical for femora of non-iguanodontian ornithopods (Norman et al., 2004). The femoral head is separated from the greater trochanter by a saddle-shaped fossa trochanteris as in some non-iguanodontian ornithopods (Han et al., 2012). The finger-like lesser trochanter is anterolaterally situated relative to the greater trochanter and terminates well below the level of the greater trochanter. On the anteromedial surface of the left femur, between the fourth trochanter and the femoral head, is a sharp-edged, circular pit with a V-shaped cross-section, distinctive of modern crocodylian feeding traces ('bisected pits') (Njau and Blumenschine, 2006). This pit is distinct from the depression for the *m. caudofemoralis longus*, which occurs at the base of and extends onto the posterior surface of the fourth trochanter (Fig. 19; Supplementary Fig. 4; Supplementary Data, Fig. S34).

The tibia is proportionately elongate and gracile (43 mm long, 10 mm in mid-length circumference, 8 mm in both proximal and distal widths), which appears to be similar to the South American ornithopod *Notohypsilophodon comodorensis* (see Fig. 9A in Ibiricu et al. 2014). Both of which are significantly more elongate than *Hypsilophodon* (Galton, 1974), *Anabisetia* (Museo Municipal "Carmen Funes", Plaza Huincul, Neuquén, Argentina ([MCF-PVPH] −74), and most North American parksosaurids, such as *Parksosaurus* and *Thescelosaurus* (Galton, 1974). The gracile proportions

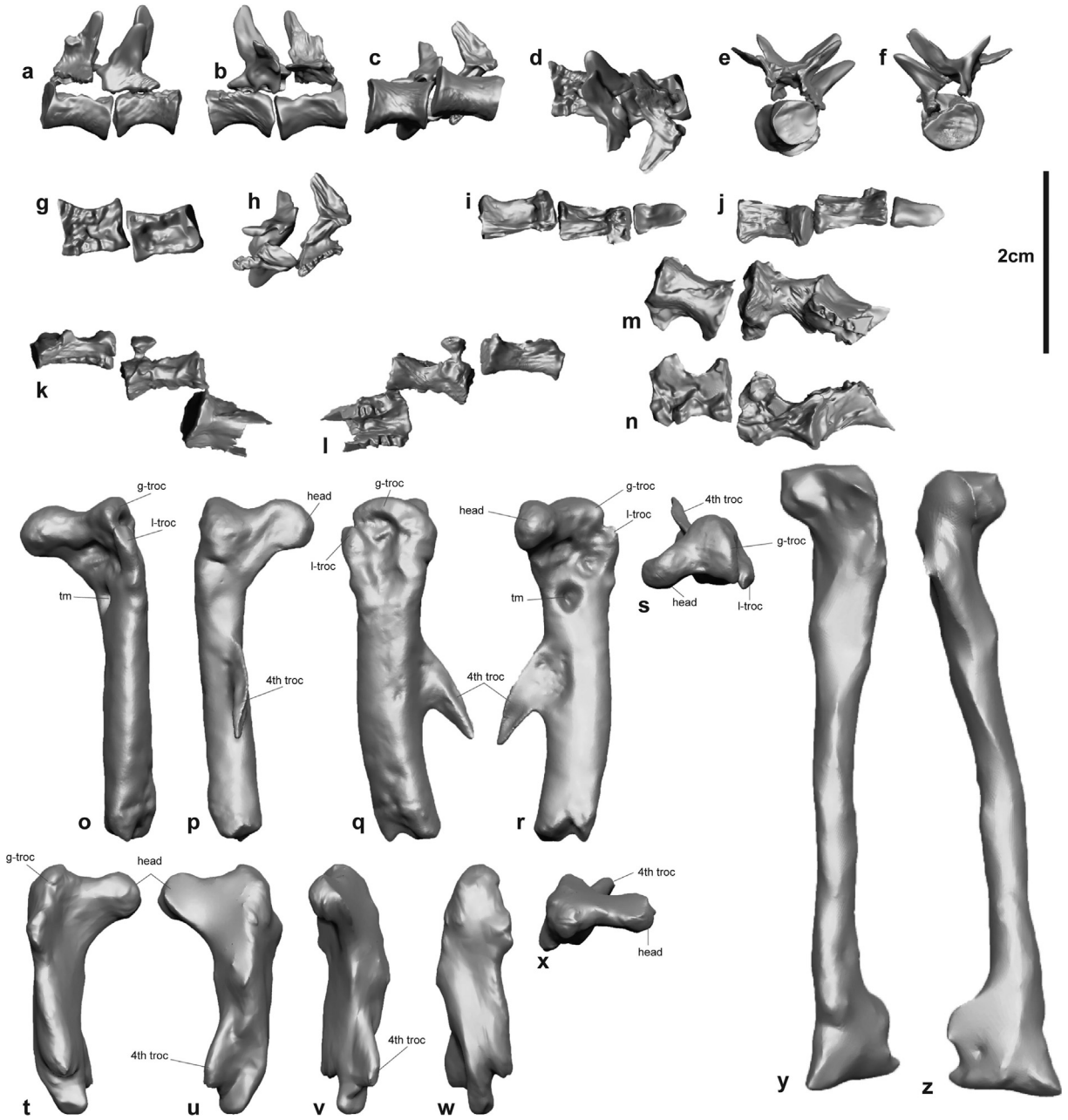

Fig. 19. Ornithopod elements found within the abdominal region of *Confractosuchus sauroktonos*. Articulated thoracic vertebrae in: (a) left lateral; (b) right lateral; (c) ventral; (d) dorsal; (e) anterior; (f) posterior; (g) dorsal view with neural spines removed; (h) ventral view of unfused neural spines. Articulated distal caudal centra in: (i) dorsal aspect; (j) ventral views. Semi-articulated last thoracic and first two sacral vertebrae in: (k) left lateral; (l) ventral; (m) right lateral; (n) dorsal aspects. Left femur in: (o) lateral, (p) medial, (q) posterior, (r) anterior, (s) proximal. Right femur in: (t) lateral, (u) medial, (v) anterior, (w) posterior, (x) proximal. Right tibia in: (y) anterior, (z) posterior. Abbreviations: g-troc, greater trochanter; l-troc, lesser trochanter; tm, tooth mark; head, femur head; 4th-troc, fourth trochanter.

might be distinctive of this taxon but might also be a result of, or exaggerated by its small size.

Comparably complete Australian ornithopod tibiae have yet to be described, therefore meaningful comparisons cannot be made. The proximal end is anteroposteriorly expanded but otherwise poorly defined in the synchrotron scans. The distal end is mediolaterally expanded and spatulate, buttressed posteriorly by a medial malleolar ridge. The medial malleolus extends below the level of the lateral malleolus. There is no indication that the distal fibula was fused to the tibia as it is in *Albertadromeus* and heterodontosaurids (Galton, 1974) (Fig. 19).

4. Phylogenetic systematics

The phylogenetic analysis produced eight most parsimonious trees of 1046 steps, and the strict consensus recovered *Confractosuchus* as an early-branching eusuchian, a sister taxon to the ancestor of susisuchids (*Isisfordia* + *Susisuchus*) and hylaeochampsids (*Hylaeochampsa* + *Iharkutosuchus* + *Acynodon*) (Fig. 20; Supplementary Data, Fig. S35). There is only one synapomorphy (calculated using the 'apo' command in TNT) diagnosing the node immediately below *Confractosuchus* (Ch. 79, Maxillary teeth waves) with the transition from state 2 (enlarged maxillary teeth curved in two waves festooned) to state 1 (one wave of teeth enlarged). This is an ambiguous synapomorphy as the same character state transition occurs between *Calsoyasuchus* and the ancestral node that it shares with *Eutretauranosuchus*.

The bootstrap and jack-knife support values for the majority of nodes within Eusuchia, including the node immediately basal to *Confractosuchus*, were very low (i.e., single digit or negative Group present/contradicted (GC) clade frequencies, see Supplementary Data, Fig. S35). These low values indicate that there is considerable uncertainty regarding the interrelationships of Eusuchia, including *Confractosuchus*, given the present cladistic dataset. Resolving the issue of poor nodal support in Eusuchia requires reconsideration of character construction in crocodyliform cladistic matrices which is beyond the scope of the present study.

5. Geometric morphometric analysis

The relative completeness of AODF 0890 enabled us to evaluate its ecomorphology via GM analysis of its skull shape. Two cranial morphometric datasets were used 1) the 3D dataset of Piras et al. (2014) (Supplementary Data, Fig. 1) and 2) 2D dataset of Drumheller & Wilberg (2019)—both of these datasets generate reliable indicators of feeding behaviour and diet in extant species (Erickson et al., 2012; Walmsley et al., 2013; Piras et al., 2014; Molnar et al., 2015; Drumheller and Wilberg, 2019)—including extant and fossil crocodyliforms. Preference was given to the 2D dataset, as it includes a broader taxonomic sampling of both extinct and extant taxa (130 vs. 26 species, respectively). Furthermore, Drumheller & Wilberg's (2019) dataset allows for a more refined dietary categorization of *Confractosuchus*, as the dataset was specifically constructed to identify such categories among crocodyliformes. Following the standard generalized Procrustes analysis, whereby landmark configurations were standardized (rotated, translated, and scaled), a principal component analysis revealed 87.9% of the variation along the first two principal component axes (Table 1). As in Drumheller and Wilberg (2019), PC1 (69.9% of the variation) describes short to long snouts and, more generally, long/narrow to short/wide crania. In comparison, PC2 (18.1% of the variation) describes wide to narrow snouts, along with relatively small to large supratemporal fossae. *Confractosuchus* occurs within the range of macro-generalists along PC1 and PC2, but also spans brevirostrine heterodont, ziphodont, and stenorostrine categories along PC2. Other crocodylians in close proximity to *Confractosuchus* include: *Theriosuchus guimarote* (fossil, macro-generalist, Late Jurassic), *Osteolaemus osborni* (extant, generalist, Congo Dwarf Crocodile), *Osteolaemus tetraspis* (extant, macro-generalist, Dwarf Crocodile), *Bernissartia* (fossil, generalist, Early Cretaceous, Laurasia), *Araripesuchus wegeneri* (fossil, brevirostrine Heterodont, Late Cretaceous).

Interestingly, *Isisfordia duncani* approaches the average crocodyliform cranial shape along PC1 and PC2 (i.e., near the origin), given this dataset. *Confractosuchus* is well placed amid the generalist category and on the edge of the ziphodont group, of

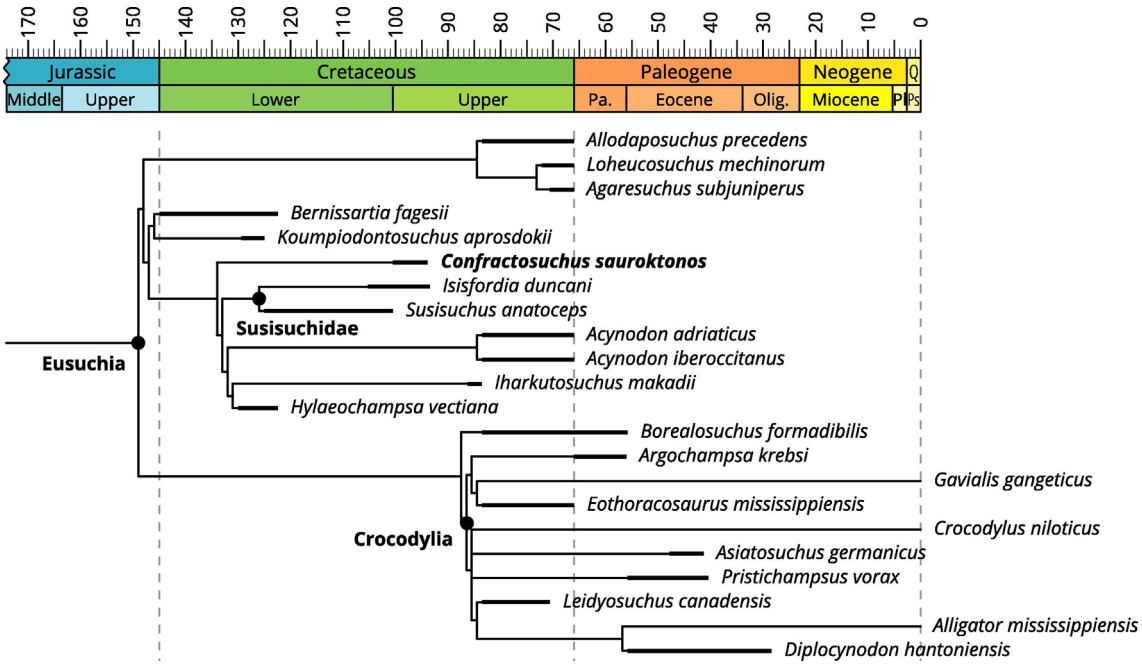

Fig. 20. Phylogenetic position of *Confractosuchus sauroktonos* gen. et sp. nov. within Eusuchia. Time-calibrated strict consensus of the 8 MPTs resulting from the analysis of the modified matrix of Martin et al. (2020), highlighting the position of *Confractosuchus sauroktonos* gen. et sp. nov. within Eusuchia.

Table 1
Results of the geometric morphometric analysis using the data from Drumheller & Wilberg (2019), showing the variance explained across the first 10 principal components.

	PC1	PC2	PC3	PC4	PC5	PC6	PC7	PC8	PC9	PC10
Standard deviation	0.15	0.076	0.031	0.028	0.026	0.02	0.018	0.014	0.011	0.009
Proportion of Variance	0.699	0.181	0.03	0.025	0.022	0.013	0.01	0.006	0.004	0.003
Cumulative Proportion	0.699	0.879	0.91	0.935	0.956	0.969	0.979	0.985	0.988	0.991

which *Isisfordia* could also belong, given its labiolingually-flattened dentition (Salisbury et al., 2006). The results indicate, at minimum, a generalist feeding lifestyle for *Confractosuchus* (Fig. 21).

6. Discussion

Confractosuchus is only the second extinct crocodyliform so far discovered with identifiable abdominal contents (see also Godoy et al., 2014) and the first to include indisputably dinosaurian remains. The ornithopod's estimated body mass (1.0–1.7 kg; calculated using the bipedal formula of Campione et al. (2014)) falls well within the size range for expected prey (Njau and Blumenschine, 2006) of *Confractosuchus*, which has an estimated body length of 2.5 m based on the preserved elements. Yet, despite its last meal, *Confractosuchus* was likely not a dinosaur specialist. The results of the GM analysis indicate that *Confractosuchus* was a macro-generalist, and, by definition, capable of taking prey larger than itself (Fig. 21). Like living platyrostral crocodylians (Grigg and Kirshner, 2015), we postulate that *Confractosuchus* was a more opportunistic feeder than is indicated by its abdominal contents.

The skeletal remains of an early-diverging ornithopod found within the abdominal cavity of *Confractosuchus* complement the sparse ornithopod record from the Winton Formation, which includes footprints and a single shed tooth (Hocknull and Cook, 2008). The gracile proportions of the tibia may be an indication that it represents a novel taxon. However, this may be a result of its small size and/or juvenile status, and comparative elements of other Australian early-branching ornithopods have not been described. As it contains no clear autapomorphies, we refrain from naming it. Unlike most iguanodontians, but in common with many early-branching ornithopods, the femur is bowed in lateral view, has a deep fossa trochanteris, and the fourth trochanter is pendent and proximally positioned (Norman, 2004; Norman et al., 2004; Butler et al. 2011; Madzia, Boyd and Mazuch, 2018). We therefore identify it as a non-iguanodontian ornithopod.

Partial articulation and absence of acid etching indicates the carcass had not been significantly digested. Stomach acids in modern crocodylians are among the most powerful in the animal kingdom (Grigg and Kirshner, 2015), which, if also true of their early-branching relatives, indicates that *Confractosuchus* died not long after its last meal. This time-of-death is supported by the articulation of some of the ingested vertebrae. However, whether *Confractosuchus* had a highly acidic gut, characteristic of living crocodiles, remains equivocal, and its effect on ingested remains, particularly during the earliest phases of digestion, cannot be disentangled from short residence time in the digestive tract (Cott, 1961; Fisher, 1981). There is, however, clear evidence of oral processing, carcass reduction (dismemberment) and bone fragmentation of the ornithopod carcass (Fig. 3; Supplementary Data, Fig. S4), which are diagnostic hallmarks of modern crocodylian feeding behaviour (Drumheller and Brochu, 2016). Crocodylians typically reduce the size of large carcasses into more manageable components using easily grasped body parts (such as the fore- and hindlimbs), which are then torn free and ingested, often as entire units (Njau and Blumenschine, 2006). Smaller prey require less reduction, enabling the pelvic girdle and limbs to be ingested directly (Njau and Blumenschine, 2006). This pattern of prey reduction appears superficially congruent with the remains found in *Confractosuchus*.

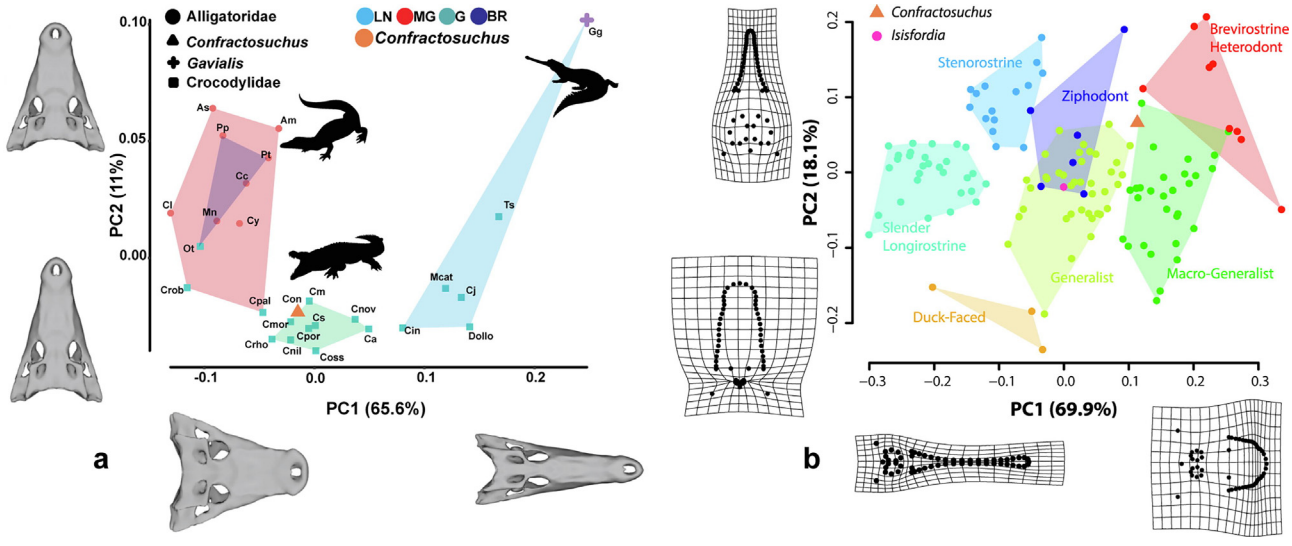

Fig. 21. Comparative cranial morphospace defined by principal components (PC) 1 (69.9% of variance) and 2 (18.1% of variance). (a), Digitized landmarks of *Confractosuchus sauroktonos* gen. et sp. nov. plotted amongst the data of Piras et al. (2014) as a principal component analysis (PCA) was used to visualize the ordination of the aligned specimens. (b), Dataset is from Drumheller & Wilberg (2019), incorporating *Confractosuchus* here plotting just within macro-generalists (can take prey larger than themselves) and *Isisfordia,* here plotting amongst generalists (can take prey equal to own body size). Abbreviations: Am, *Alligator mississippiensis*; As, *Alligator sinensis*; Ca, *Crocodylus acutus;* Cc, *Caiman crocodylus*; Cin, *Crocodylus intermedius*; Cj, *Crocodylus johnstoni*; Cl, *Caiman latirostris*; Cm, *Crocodylus mindorensis*; Cmor, *Crocodylus moreletii*; Cnil, *Crocodylus niloticus*; Cnov, *Crocodylus novaeguineae*; Coss, *Crocodylus ossifragus*; Cpal, *Crocodylus palustris*; Cpor, *Crocodylus porosus*; Crho, *Crocodylus rhombifer*; Crob, *Voay robustus*; Cs, *Crocodylus siamensis*; Cy, *Caiman yacare*; Con, *Confractosuchus sauroktonos*; Dollo, *Dollosuchoides densmorei*; Gg, *Gavialis gangeticus;* Mcat, *Mecistops cataphractus*; Mn, *Melanosuchus niger*; Ot, *Osteolaemus tetraspis*; Pp, *Paleosuchus palpebrosus*; Pt, *Paleosuchus trigonatus*; Ts, *Tomistoma schlegelii.* LN, longirostrine; MG, macro-generalist; G, generalist; BR, brevirostrine.

Although it is possible that the juvenile ornithopod was scavenged, given its small size in relation to its consumer, there is an equally likely but currently untestable probability that it suffered a crocodylian-style ambush feeding strategy (Njau and Blumenschine, 2006; Gody et al., 2014). However, the abdominal region preserving the ornithopod was badly damaged by excavation equipment prior to its discovery, hindering its overall restoration; it is uncertain how much of the ornithopod was initially preserved. Post-mortem decay and disarticulation of *Confractosuchus* prior to burial may have also reduced the preservation of the entire abdominal cavity.

The shift from Neosuchia to Eusuchia is one of the key transitions in crocodyliform evolution, as it represents the onset of the modern crocodylian *bauplan* (Salisbury et al., 2006; Turner and Pritchard, 2015; Leite and Fortier, 2018) together with the adoption of a strictly semi-aquatic, ambush-predator lifestyle (Gignac and O'Brien, 2016). Historically, this transition simultaneously centred on the position and construction of the choana and the acquisition of procoelous vertebrae (Salisbury et al., 2006; Turner and Pritchard, 2015; Leite and Fortier, 2018). Interestingly, despite the poor nodal support within Eusuchia, the position and construction of the choana (bound by palatines and pterygoids) of *Confractosuchus* support its phylogenetic position in relation to Susisuchidae, which possess a pterygoid-bound choana. However, these characters have been found to vary more widely in early-branching eusuchians and their closest relatives (hylaeochampsids, bernissartiids and susisuchids) (Martin et al., 2020). Despite this, *Confractosuchus* is recovered within a group consisting of mostly highly derived neosuchians and the construction of its choana and varying vertebrae morphologies supports its phylogenetic position.

Finally, the vertebral arrangement in *Confractosuchus* demonstrates that the acquisition of procoelous vertebrae was not universally acquired. Its presence in the neck region but lack thereof in the majority of the trunk, indicates there was likely some structural advantage to its acquisition in this region initially. Interestingly, crocodyliforms with fully segmented paravertebral shields and amphicoelous vertebrae, were small (e.g., *Susisuchus*), because they lacked the structural support of a paravertebral shield that reinforced the trunk against shear loads associated with terrestrial locomotion (Molnar et al. 2015; Salisbury and Frey, 2001; Salisbury et al., 2006). Furthermore, in extant crocodylians, the acquisition of procoelous vertebrae along with horizontally-oriented zygapophyses created a rigid bracing system and allowed for a more flexible arrangement of the paravertebral shield (Salisbury and Frey 2001; Molnar et al. 2015). This structural arrangement provided the structural support necessary for sustained terrestrial locomotion in all extant forms and afforded a greater range of motion concordant with a semi-aquatic lifestyle (Molnar et al., 2015). If procoelous vertebrae evolved to cope with increased shear loads, its presence in the neck and lack thereof in the majority of the trunk, indicates the neck region was initially reinforced. Therefore, we hypothesise that these characteristics, coupled with a fully segmented paravertebral shield, facilitated aquatic ambush-style predatory behaviour by enabling greater flexibility and a strengthened neck region to dispatch and dismember struggling prey (Njau and Blumenschine, 2006; Molnar et al., 2015; Fish et al., 2007), such as juvenile dinosaurs.

Confractosuchus represents only the second Crocodyliform discovered from the Winton Formation. The other, *Isisfordia duncani*, comprises multiple semi-articulated and partially complete skeletons, and assigned isolated elements, all of which come from potentially lower parts of the formation than *Confractosuchus* (Salisbury et al., 2006; Syme & Salisbury, 2018). Isolated crocodyliform fossils and, more recently, traces (Poropat et al., 2021), are quite common, having been discovered at nearly all of the AODL's, including over 40 teeth discovered at one locality (AODL0127). Descriptions of these isolated elements and teeth are beyond the scope of this publication, but their abundance indicates that crocodyliforms were common predators of the mid-Cretaceous freshwater fluvial and lacustrine ecosystems of the Winton Formation.

7. Conclusion

Here, we have described a new crocodyliform, *Confractosuchus sauroktonos* gen. et sp. nov., from the Winton Formation of central Queensland Australia. Its last meal, a juvenile ornithopod dinosaur, was discovered in its abdominal cavity. These gut contents oddly represent the first recorded skeletal remains of ornithopods from the Winton Formation and may represent a novel taxon. The abdominal contents provided a unique opportunity to verify predictions of feeding behaviour, ascertained from a morphometric analysis of the skull. The prediction of *Confractosuchus* as a macro-generalist or, at the very least a generalist feeder via GM was substantiated by the ornithopod it consumed.

Declaration of Competing Interest

The authors declare that they have no known competing financial interests or personal relationships that could have appeared to influence the work reported in this paper.

Acknowledgements

We thank the Australian Age of Dinosaurs Museum staff and volunteers for coordinating the excavation of this specimen; Bob Elliott, Sandra Muir and Ian Muir for the specimens discovery; Judy Chelini and Judy Elliott for the specimen preparation. We thank Dr. Paolo Piras for his suggestions on the GMM part of this study. We thank Dr Adam Pritchard, Dr Keegan Melstrom for reviewing initial drafts of this manuscript. We thank the two anonymous reviewers and Dr Joseph Meert for their constructive feedback. TNT is made freely available thanks to a subsidy from the Willi Hennig Society. This work was supported by a University of New England Internal Scholarship to (MAW). The Australian Nuclear Science and Technology Organisation access grants to MAW, JJB, DAE (AS183/IMBL/M13963) M10862, M9508, ACN/DINGO/P4371, P3977, DB6552, IC3802). The Australian Research Council Discovery Early Career Researcher Awards to NEC (project ID: DE190101423) and PRB (project ID: DE170101325).

Appendix A. Supplementary data

Supplementary data to this article can be found online at https://doi.org/10.1016/j.gr.2022.01.016.

References

Adams, D.C., Collyer, M.L., 2019. Geomorph: Software for geometric morphometric analyses, Version 3.1.0. R Package (CRAN).

Benton, M.J., Clark, J.M., 1988. Archosaur phylogeny and the relationships of the Crocodylia. In: Benton, M.J., (Ed), The Phylogeny and Classification of Tetrapods, Vol 1. Amphibians, Reptiles, Birds. Oxford, Clarendon Press, 296–338.

Blanco, A., Puértolas-Pascual, E., Marmi, J., Vila, B., Sellés, A.G., Dodson, P., 2014. *Allodaposuchus palustris* sp. nov. from the upper Cretaceous of Fumanya (Southeastern Pyrenees, Iberian Peninsula): systematics, palaeoecology and palaeobiogeography of the enigmatic allodaposuchian crocodylians. PLoS ONE 9 (12), e115837. https://doi.org/10.1371/journal.pone.0115837.

Blanco, A., Fortuny, J., Vicente, A., Luján, À.H., García-Marçà, J.A., Sellés, A.G., 2015. A new species of *Allodaposuchus* (Eusuchia, Crocodylia) from the Maastrichtian (Late Cretaceous) of Spain: phylogenetic and paleobiological implications. PeerJ 3, e1171. https://doi.org/10.7717/peerj.1171.

Boyd, C.A., Drumheller, S.K., Gates, T.A., Farke, A.A., 2013. Crocodyliform feeding traces on juvenile ornithischian dinosaurs from the Upper Cretaceous (Campanian) Kaiparowits Formation. Utah. PLoS ONE 8 (2), e57605. https://doi.org/10.1371/journal.pone.0057605.
Brochu, C.A., 1996. Closure of neurocentral sutures during crocodilian ontogeny: implications for maturity assessment in fossil archosaurs. J. Vertebr. Paleontol. 16 (1), 49–62.
Brochu, C.A., 1999. Phylogenetics, taxonomy and historical biogeography of Alligatoroidea. Society of Vertebrate Paleontology, Memoir 6. J. Vertebr. Paleontol. 19 (sup002), 9–100.
Brochu, C.A., 2007a. Morphology, relationships and biogeographic significance of an extinct horned crocodile (Crocodylia, Crocodylidae) from the Quaternary of Madagascar. Zool. J. Linn. Soc. 150, 835–63.
Brochu, C.A., 2007b. Systematics and taxonomy of Eocene tomistomine crocodylians from Britain and northern Europe. Palaeontology 50 (4), 917–928.
Brown, C.M., Evans, D.C., Ryan, M.J., Russell, A.P., 2013. New data on the diversity and abundance of small-bodied ornithopods (Dinosauria, Ornithischia) from the Belly River Group (Campanian) of Alberta. J. Vertebr. Paleontol. 33 (3), 495–520.
Buckley, G.A., Brochu, C.A., Krause, D.W., Pol, D., 2000. A pug-nosed crocodyliform from the late cretaceous of Madagascar. Nature 405 (6789), 941–944.
Buscalioni, A.D., Sanz, J.L., 1990. The small crocodile *Bernissartia fagesii* from the Lower Cretaceous of Galve (Teruel, Spain). Bulletin de l'Institut Royal des Sciences Naturelles de Belgique, Sciences de la Terre. 60, 129–150.
Butler, R.J., Liyong, Jin, Jun, Chen, Godefroit, Pascal, 2011. The postcranial osteology and phylogenetic position of the small ornithischian dinosaur *Changchunsaurus parvus* from the Quantou Formation (Cretaceous: Aptian–Cenomanian) of Jilin Province, north-eastern China. Palaeontology 54 (3), 667–683.
Campione, N.E., Evans, D.C., Brown, C.M., Carrano, M.T., Revell, L., 2014. Body mass estimation in non-avian bipeds using a theoretical conversion to quadruped stylopodial proportions. Methods Ecol. Evol. 5 (9), 913–923.
Cook, A.G., Bryan, S.E., Draper, J.J., 2013. Post-orogenic Mesozoic basins and magmatism. In: Jell, P. (Ed.), Geology of Queensland. Geological Survey of Queensland, Australia, pp. 515–575.
Cott, H.B., 1961. Scientific results of an inquiry into the ecology and economic status of the Nile crocodile (*Crocodilus niloticus*) in Uganda and Northern Rhodesia. Trans. Zool. Soc. London 29, 211–356.
Dubois, E., 1908. Das Geologische alter der Kendeng-oder Trinil-fauna. Tijdschrift van het Koninklijk Nederlandsch Aardrijkskunding Genootschap 25, 1235–1270.
Drumheller, S.K., Brochu, C.A., 2016. Phylogenetic taphonomy: a statistical and phylogenetic approach for exploring taphonomic patterns in the fossil record using crocodylians. Palaios 31 (10), 463–478.
Drumheller, S.K., Wilberg, E.W., 2019. A synthetic approach for assessing the interplay of form and function in the crocodyliform snout. Zool. J. Linn. Soc. 188, 507–521.
Erickson, G.M., Gignac, P.M., Steppan, S.J., Lappin, A.K., Vliet, K.A., Brueggen, J.D., Inouye, B.D., Kledzik, D., Webb, G.J.W., Claessens, L., 2012. Insights into the ecology and evolutionary success of crocodilians revealed through bite-force and tooth-pressure experimentation. PLoS ONE 7 (3), e31781. https://doi.org/10.1371/journal.pone.0031781.
Figueiredo, R.G., Moreira, J.K.R., Saraiva, A.A.F., Kellner, A.W., 2011. A description of a new specimen of *Susisuchus anatoceps* (Crocodylomorpha: Mesoeucrocodylia) from the Crato Formation (Santana Group) with comments on Neosuchia. Zool. J. Linn. Soc. 163, 273–288.
Fish, F.E., Bostic, S.A., Nicastro, A.J., Beneski, J.T., 2007. Death roll of the alligator: mechanics of twist feeding in water. J. Exp. Biol. 210, 2811–2818.
Fisher, D.C., 1981. Crocodilian scatology, microvertebrate concentrations, and enamel-less teeth. Paleobiology 7 (2), 262–275.
Galton, P.M., 1974. The ornithischian dinosaur *Hypsilophodon* from the Wealden of the Isle of Wight. Bulletin of the British Museum (Natural History). Geology 25, 1–152.
Garbe, U., Randall, T., Hughes, C., Davidson, G., Pangelis, S., Kennedy, S.J., 2015. A new neutron radiography / tomography / imaging station DINGO at OPAL. Phys. Procedia. 69, 27–32.
Gignac, P., O'Brien, H., 2016. Suchian feeding success at the interface of ontogeny and macroevolution. Integr. Comp. Biol. 56 (3), 449–458.
Godoy, P.L., Montefeltro, F.C., Norell, M.A., Langer, M.C., Viriot, L., 2014. An additional baurusuchid from the Cretaceous of Brazil with evidence of interspecific predation among crocodyliformes. PLoS ONE 9 (5), e97138. https://doi.org/10.1371/journal.pone.0097138.
Goloboff, P.A., Catalano, S.A., 2016. TNT version 1.5, including a full implementation of phylogenetic morphometrics. Cladistics 32, 221–238.
Grigg, G.C., Kirshner, D., 2015. Biology and Evolution of Crocodylians. CSIRO Publishing, 230–234.
Han, F.-L., Barrett, P.M., Butler, R.J., Xu, X., 2012. Postcranial anatomy of *Jeholosaurus shangyuanensis* (Dinosauria, Ornithischia) from the Lower Cretaceous Yixian Formation of China. J. Vertebr. Paleontol. 32 (6), 1370–1395.
Hart, L.J., Bell, P.R., Smith, E.T., Mitchell, D.R., Birch, S.A., Salisbury, S.W., 2021. A probable skeleton of *Isisfordia* (Crocodyliformes) and additional crocodyliform remains from the Griman Creek Formation (Cenomanian, New South Wales, Australia). J. Paleontol. 95 (2), 351–366.
Hay, O.P., 1930. Second bibliography and catalogue of the fossil vertebrata of North America 2. Carnegie Institute Washington, Washington, DC.
Hocknull, S.A., Cook, A.G., 2008. Hypsilophodontid (Dinosauria: Ornithischia) from the latest Albian, Winton Formation, central Queensland. Mem. Qld. Mus. 52, 212.
Hocknull, S.A., White, M.A., Tischler, T.R., Cook, A.G., Calleja, N.D., Sloan, T., Elliott, D. A., Sereno, P., 2009. New mid-Cretaceous (latest Albian) dinosaurs from Winton, Queensland. Australia. PLoS ONE 4 (7), e6190. https://doi.org/10.1371/journal.pone.0006190.
Hocknull, S.A., Wilkinson, M., Lawrence, R.A., Konstantinov, V., Mackenzie, S., Mackenzie, R., 2021. A new giant sauropod, *Australotitan cooperensis* gen. et sp. nov., from the mid-Cretaceous of Australia. PeerJ 9, e11317. https://doi.org/10.7717/peerj.11317.
Hu, Y., Meng, J., Wang, Y., Li, C., 2005. Large Mesozoic mammals fed on young dinosaurs. Nature 433 (7022), 149–152.
Huxley, T.H., 1875. On *Stagonolepis robertsoni*, and on the evolution of the Crocodilia. J. Geol. Soc. London. 31 (1-4), 423–438.
Ibiricu, L.M., Martínez, R.D., Luna, M., Casal, G.A., 2014. A reappraisal of *Notohypshilophodon comodorensis* (Ornithischia: Ornithopoda) from the Late Cretaceous of Patagonia, Argentina. Zootaxa 3786, 401–422.
Klinkhamer, A.J., Wilhite, D.R., White, M.A., Wroe, S., Claessens, L., 2017. Digital dissection and three-dimensional interactive models of limb musculature in the Australian estuarine crocodile (*Crocodylus porosus*). PLoS ONE 12 (4), e0175079. https://doi.org/10.1371/journal.pone.0175079.
Langston, W., Rose, H., 1978. A yearling crocodilian from the Middle Eocene Green River Formation of Colorado. J. Paleontol. 52, 122–125.
Leite, K.J., Fortier, D.C., 2018. The palate and choanae structure of the *Susisuchus anatoceps* (Crocodyliformes, Eusuchia): phylogenetic implications. PeerJ 6, e5372. https://doi.org/10.7717/peerj.5372.
Madzia, D., Boyd, C.A., Mazuch, M., 2018. A basal ornithopod dinosaur from the Cenomanian of the Czech Republic. J. Syst. Palaeontol. 16 (11), 967–979.
Martin, J.E., Delfino, M., Smith, T., 2016. Osteology and affinities of Dollo's Goniopholidid (Mesoeucrocodylia) from the Early Cretaceous of Bernissart. Belgium. J. Vertebr. Paleontol. 36 (6), e1222534. https://doi.org/10.1080/02724634.2016.1222534.
Martin, J.E., Smith, T., Salaviale, C., Adrien, J., Delfino, M., 2020. Virtual reconstruction of the skull of *Bernissartia fagesii* and current understanding of the neosuchian–eusuchian transition. J. Syst. Palaeontol. 18 (13), 1079–1101.
Mays, C., Bevitt, J., Stilwell, J., 2017. Pushing the limits of neutron tomography in palaeontology: Three-dimensional modelling of in situ resin within fossil plants. Palaeontol. Electron. 201720, 57A.
Melstrom, K.M., Irmis, R.B., 2019. Repeated evolution of herbivorous crocodyliforms during the age of dinosaurs. Curr. Biol. 29 (14), 2389–2395.e3.
Molnar, R.E., Galton, P.M., 1986. Hypsilophodontid dinosaurs from Lightning Ridge, New South Wales, Australia. Geobios 19 (2), 231–243.
Molnar, J.L., Pierce, S.E., Bhullar, B.-A., Turner, A.H., Hutchinson, J.R., 2015. Morphological and functional changes in the vertebral column with increasing aquatic adaptation in crocodylomorphs. Royal Soc. Open Sci. 2 (11), 150439. https://doi.org/10.1098/rsos.150439.
Narváez, I., Brochu, C.A., Celis, A., Codrea, V., Escaso, F., Pérez-García, A., Ortega, F., 2020. New diagnosis for *Allodaposuchus precedens*, the type species of the European Upper Cretaceous clade Allodaposuchidae. Zool. J. Linn. Soc. 189, 618–634.
Narváez, I., Brochu, C.A., Escaso, F., Pérez-García, A., Ortega, F., Smith, T., 2015. New Crocodyliforms from Southwestern Europe and Definition of a Diverse Clade of European Late Cretaceous Basal Eusuchians. PLoS ONE 10 (11), e0140679. https://doi.org/10.1371/journal.pone.0140679.
Njau, J.K., Blumenschine, R.J., 2006. A diagnosis of crocodile feeding traces on larger mammal bone, with fossil examples from the Plio-Pleistocene Olduvai Basin. Tanzania. J. Hum Evol. 50 (2), 142–162.
Norman, D.B., 2004. Basal Iguanodontia. In: Weishampel, D.B., Dodson, P., Osmolska, H. (Eds.), The Dinosauria. second edition. University California Press, Berkeley, pp. 413–437.
Norman, D.B., Sues, H.-D., Witmer, L.M., Coria, R.A., 2004. Basal Ornithopoda. In: Weishampel, D.B., Dodson, P., Osmolska, H. (Eds.), The Dinosauria. second edition. University California Press, Berkeley, pp. 393–412.
Noto, C.R., Main, D.J., Drumheller, S.K., 2012. Feeding traces and paleobiology of a Cretaceous (Cenomanian) crocodyliform: example from the Woodbine Formation of Texas. Palaios 27 (2), 105–115.
Piras, P., Buscalioni, A.D., Teresi, L., Raia, P., Sansalone, G., Kotsakis, T., Cubo, J., 2014. Morphological integration and functional modularity in the crocodilian skull. Integr. Zool. 9, 498–516.
Poropat, S.F., White, M.A., Ziegler, T., Pentland, A.H., Rigby, S.L., Duncan, R.J., Sloan, T., Elliott, D.A., 2021. A diverse Late Cretaceous vertebrate tracksite from the Winton Formation of Queensland. Australia. PeerJ 9, e11544. https://doi.org/10.7717/peerj.11544.
Rich, T.H., Vickers-Rich, P., 1989. Polar dinosaurs and biotas of the Early Cretaceous of southeastern Australia. Natl. Geogr. Res. 5, 15–53.
Rich, T.H., Vickers-Rich, P., 1999. The Hypsilophodontidae from southeastern Australia. In: Tomida, Y., Rich, T.H., Vickers-Rich, P. (Eds.), Proceedings of the Second Gondwanan Dinosaur Symposium. National Science Museum.
Rivera-Sylva, H.E., Frey, E., Guzmán-Gutiérrez, J.R., 2009. Evidence of predation on the vertebra of a hadrosaurid dinosaur from the Upper Cretaceous (Campanian) of Coahuila. Mexico. Carnets Geol. CG2009 (L02), 1–6.
Rogers, J.V., 2003. *Pachycheilosuchus trinquei*, a new procoelous crocodyliform from the Lower Cretaceous (Albian) Glen Rose Formation of Texas. J. Vertebr. Paleontol. 23 (1), 128–145.
Rohlf, F.J., 2018 TpsDig2; Version 2.31. Stony Brook.
Salgado, L., Coria, R.A., Heredia, S.E., 1997. New materials of *Gasparinisaura cincosaltensis* (Ornithischia, Ornithopoda) from the Upper Cretaceous of Argentina. J. Paleontol. 71 (5), 933–940.

Salisbury, S.W., Frey, E.F., 2001. A biomechanical transformation model for the evolution of semi-spheroidal articulations between adjoining vertebral bodies in crocodilians. In: Grigg, G.C., Seebacher, F., Franklin, C.E. (Eds.), Crocodilian biology and evolution. Surry Beatty and Sons, Chipping Norton, Australia, pp. 85–134.

Salisbury, S.W., Frey, E., Martill, D.M., Buchy, M.-C., 2003. A new crocodilian from the Lower Cretaceous Crato Formation of north-eastern Brazil. Palaeontogr. Abt. A. 270 (1-3), 3–47.

Salisbury, S.W., Molnar, R.E., Frey, E., Willis, P.M.A., 2006. The origin of modern crocodyliforms: new evidence from the Cretaceous of Australia. Proc. Royal Soc. B. 273 (1600), 2439–2448.

Scheetz, R.D., 1999. Osteology of *Orodromeus makelai* and the phylogeny of basal ornithopod dinosaurs. Montana State University, Bozeman, p. 186. Ph.D thesis.

Schlager, S., 2013. Morpho: Calculations and visualizations related to Geometric Morphometrics. R package version (23), 3.

Schwimmer, D.R., 2002. King of the crocodylians: The Paleobiology of *Deinosuchus*. Indiana University Press, Bloomington, Indiana, pp. 1–220.

Sellés, A.G., Blanco, A., Vila, B., Marmi, J., López-Soriano, F.J., Llácer, S., Frigola, J., Canals, M., Galobart, À., 2020. A small Cretaceous crocodyliform in a dinosaur nesting ground and the origin of sebecids. Sci. Rep. 10 (1). https://doi.org/10.1038/s41598-020-71975-y.

Sereno, P.C., Larsson, H.C.E., Sidor, C.A., Gado, B., 2001. The giant crocodyliform *Sarcosuchus* from the Cretaceous of Africa. Science 294, 1516–1519.

Simpson, G.G., 1944. Tempo and Mode in Evolution. Columbia University Press, New York.

Syme, C.E., Salisbury, S.W., 2018. Taphonomy of *Isisfordia duncani* specimens from the Lower Cretaceous (upper Albian) portion of the Winton Formation, Isisford, central-west Queensland. R. Soc. Open Sci. 5 (3), 171651. https://doi.org/10.1098/rsos.171651.

Syme, C.E., Salisbury, S.W., 2014. Patterns of aquatic decay and disarticulation in juvenile Indo-Pacific crocodiles (*Crocodylus porosus*), and implications for the taphonomic interpretation of fossil crocodyliform material. Palaeogeogr. Palaeocl Palaeoecol. 412, 108–123.

Tucker, R.T., Roberts, E.M., Darlington, V., Salisbury, S.W., 2017. Investigating the stratigraphy and palaeoenvironments for a suite of newly discovered mid-Cretaceous vertebrate fossil-localities in the Winton Formation, Queensland. Australia. Sediment. Geol. 358, 210–229.

Tucker, R.T., Roberts, E.M., Henderson, R.A., Kemp, A.I., 2016. Late igneous province or long-lived magmatic arc along the eastern margin of Australia during the Cretaceous? Insights from the sedimentary record. GSA Bulletin. 128, 1461–1480.

Tucker, R.T., Roberts, E.M., Hu, Y.i., Kemp, A.I.S., Salisbury, S.W., 2013. Detrital zircon age constraints for the Winton Formation, Queensland: contextualizing Australia's Late Cretaceous dinosaur faunas. Gondwana Res. 24 (2), 767–779.

Turner, A.H., Dodson, P., 2015. A Review of *Shamosuchus* and *Paralligator* (Crocodyliformes, Neosuchia) from the Cretaceous of Asia. PLoS ONE 10 (2), e0118116. https://doi.org/10.1371/journal.pone.0118116.

Turner, A.H., Pritchard, A.C., 2015. The monophyly of Susisuchidae (Crocodyliformes) and its phylogenetic placement in Neosuchia. PeerJ 3, e759. https://doi.org/10.7717/peerj.759.

Walmsley, C.W., Smit, P.D., Quale, M.R., McCurry, M.R., Richards, H.S., Oldfield, C.C., Wroe, S., Clausen, P.D., McHenry, C.R., 2013. Why the long face? Mechanics of mandibular symphysis proportions in crocodiles. PLoS ONE 8, (1) e53873.

Whetstone, K.N., Whybrow, P.J., 1983. A 'cursorial' crocodilian from the Triassic of Lesotho (Basutoland), southern Africa. Occas. Pap. Mus. Nat. Hist. (Lawrence) 106, 1–37.

White, M.A., Bell, P.R., Poropat, S.F., Pentland, A.H., Rigby, S.L., Cook, A.G., Sloan, T., Elliott, D.A., 2020. New theropod remains and implications for megaraptorid diversity in the Winton Formation (lower Upper Cretaceous) Queensland. Australia. Roy. Soc. Open. Sci. 7 (1), 191462. https://doi.org/10.1098/rsos.191462.

Wilson, J.A., Mohabey, D.M., Peters, S.E., Head, J.J., Benton, M.J., 2010. Predation upon hatchling dinosaurs by a new snake from the Late Cretaceous of India. PLoS Biol. 8 (3), e1000322. https://doi.org/10.1371/journal.pbio.1000322.